

ESCOLA POLITÉCNICA
PROGRAMA DE PÓS-GRADUAÇÃO EM ENGENHARIA E TECNOLOGIA DE MATERIAIS
MESTRADO EM ENGENHARIA E TECNOLOGIA DE MATERIAIS

ADRIELLE DORNELLES DEWES

**CHARACTERIZATION AND EVALUATION OF ANTIBACTERIAL ACTIVITY OF THIN AND
ULTRATHIN Ag AND Cu COATINGS DEPOSITED ON GLASS SUBSTRATES VIA
MAGNETRON SPUTTERING**

Porto Alegre

2022

PÓS-GRADUAÇÃO - *STRICTO SENSU*



Pontifícia Universidade Católica
do Rio Grande do Sul



Pontifícia Universidade Católica do Rio Grande do Sul

ESCOLA POLITÉCNICA

PROGRAMA DE PÓS-GRADUAÇÃO EM ENGENHARIA E TECNOLOGIA DE MATERIAIS

**CARACTERIZAÇÃO E AVALIAÇÃO DA ATIVIDADE
ANTIBACTERIANA DE REVESTIMENTOS FINOS E ULTRAFINOS DE
Ag E Cu DEPOSITADOS EM SUBSTRATO DE VIDRO VIA
*MAGNETRON SPUTTERING***

**CHARACTERIZATION AND EVALUATION OF ANTIBACTERIAL
ACTIVITY OF THIN AND ULTRATHIN Ag AND Cu COATINGS
DEPOSITED ON GLASS SUBSTRATES VIA MAGNETRON
SPUTTERING**

ADRIELLE DORNELLES DEWES

B.SC. IN PHYSICS AND LICENSE IN PHYSICS

ORIENTADOR: PROF(a). DR(a).

CO-ORIENTADOR: Advisor: Prof. Dr. Ricardo Meurer Papaleo (ago/22 a set/22)

Prof. Dr. Adriano Friedrich Feil (abr/20 a jul/22)

Co-advisor: Prof(a). Dr(a). Sílvia Dias de Oliveira

Dissertation fulfilled in the Graduate Program in Materials Engineering and Technology (PGETEMA) at the Pontifical Catholic University of Rio Grande do Sul, as a requirement for obtaining the title of Master in Materials Engineering and Technology.

**Porto Alegre
September, 2022**

Ficha Catalográfica

D517c Dewes, Adrielle Dornelles

Characterization And Evaluation Of Antibacterial Activity Of Thin And Ultrathin Ag And Cu Coatings Deposited On Glass Substrates Via Magnetron Sputtering / Adrielle Dornelles Dewes. – 2022.

73 p.

Dissertação (Mestrado) – Programa de Pós-Graduação em Engenharia e Tecnologia de Materiais, PUCRS.

Orientador: Prof. Dr. Ricardo Meurer Papaléo.

Coorientadora: Profa. Dra. Sílvia Dias de Oliveira.

1. Antibacterial Materials. 2. Silver. 3. Copper. 4. Surfaces & Coatings. 5. Surface Engineering. I. Papaléo, Ricardo Meurer. II. Oliveira, Sílvia Dias de. III. , . IV. Título.

Elaborada pelo Sistema de Geração Automática de Ficha Catalográfica da PUCRS
com os dados fornecidos pelo(a) autor(a).

Bibliotecária responsável: Clarissa Jesinska Selbach CRB-10/2051



Pontifícia Universidade Católica do Rio Grande do Sul
 ESCOLA POLITÉCNICA
 PROGRAMA DE PÓS-GRADUAÇÃO EM ENGENHARIA E TECNOLOGIA DE MATERIAIS

Characterization And Evaluation Of Antibacterial Activity Of Thin And Ultrathin Ag And Cu Coatings Deposited On Glass Substrate Via Magnetron Sputtering

CANDIDATA: ADRIELLE DORNELLES DEWES

Esta Dissertação de Mestrado foi julgada para obtenção do título de MESTRE EM ENGENHARIA E TECNOLOGIA DE MATERIAIS e aprovada em sua forma final pelo Programa de Pós-Graduação em Engenharia e Tecnologia de Materiais da Pontifícia Universidade Católica do Rio Grande do Sul.



DR. RICARDO MEURER PAPALÉO - ORIENTADOR



DRA. SILVIA DIAS DE OLIVEIRA - COORIENTADORA

BANCA EXAMINADORA



DR. LUIS GUSTAVO PEREIRA - DO PG EM FÍSICA - UFRGS



DRA. ROSANE ANGÉLICA LIGABUE - DO PGETEMA - PUCRS

PUCRS

Campus Central
 Av. Ipiranga, 6681 - Prédio 32 - Sala 507 - CEP: 90619-900
 Telefone: (51) 3353.4059 - Fax: (51) 3320.3625
 E-mail: engenharia.pg.materials@pucrs.br
 www.pucrs.br/politecnica

*“We keep moving forward,
opening new doors, and doing
new things, because we’re curious
and curiosity keeps leading us
down new paths.” (Walt Disney)*

ACKNOWLEDGEMENTS

Agradeço primeiramente aos meus pais, Liane e Mauro, por todo o suporte, cuidado e apoio. Agradeço por serem minha fonte inesgotável de inspiração e amor.

Agradeço aos meus orientadores por me auxiliarem no que foi preciso e me acompanharem durante este tempo. Agradeço também à minha coorientadora, Professora Sílvia Dias, por esclarecer minhas dúvidas e me dar todo o suporte que precisei durante o processo de pesquisa em uma área que eu não tinha muita familiaridade.

Agradeço aos meus colegas de pesquisa e aos demais professores do laboratório por toda ajuda, conversas e troca de ideias durante os longos períodos no NANOPUC.

Agradeço às técnicas do Laboratório de Imunologia e Microbiologia da PUCRS, Maila e Vanessa, por toda ajuda, paciência e ensinamentos durante os experimentos que precisei realizar. Agradeço a todos do laboratório que de alguma forma me auxiliaram em tudo que eu precisei.

Agradeço também a todos os meus amigos e família que estiveram comigo, me apoiaram e que mesmo de longe acompanham a minha trajetória.

Agradeço ao INCT-INES pelo apoio ao laboratório.

Este estudo foi financiado pela Coordenação de Aperfeiçoamento de Pessoal de Nível Superior (CAPES) pelo Programa Ação Emergencial – COVID-19.

Obrigada!

TABLE OF CONTENTS

ACKNOWLEDGEMENTS	6
TABLE OF CONTENTS	7
LIST OF FIGURES	9
LIST OF TABLES.....	11
LIST OF SYMBOLS AND ABBREVIATIONS.....	12
RESUMO.....	14
ABSTRACT.....	16
1. INTRODUCTION	17
2. OBJECTIVES.....	19
2.1. Specific Objectives	19
3. BACKGROUND	20
3.1. Viruses and Bacteria.....	20
3.2. Nanoscience and Nanotechnology	23
3.2.1. Metal Nanoparticles as Biocidal Agents	25
3.2.1.1. Silver Nanoparticles (AgNPs).....	26
3.2.1.2. Copper Nanoparticles (CuNPs).....	27
3.3. Magnetron Sputtering	28
3.4. Personal Protective Equipment (PPE).....	30
3.5. State of Art.....	30
4. MATERIALS E METHODS	33
4.1. Substrates.....	33
4.2. Metallic Deposition.....	33
4.3. Characterization Techniques	34
4.3.1. Rutherford Backscattering Spectrometry (RBS).....	34
4.3.2. Scanning Electron Microscopy (SEM).....	37
4.4. Antibacterial Evaluation.....	38
4.4.1. Contact Method.....	38
5. RESULTS AND DISCUSSION.....	41
5.1. SEM Analysis.....	41

5.2. Analysis of the Presence of Silver and Copper on the Samples.....	50
5.3. Analysis of Antibacterial test	56
5.3.1. Contact Method.....	56
6. CONCLUSIONS	61
7. PROPOSALS FOR FUTURE WORK.....	63
8. REFERENCES	64

LIST OF FIGURES

Figure 1. Schematic representation of SARS-CoV-2 structure.....	20
Figure 2. Representation of cell walls of gram-positive (a) and gram-negative (b) bacteria.....	21
Figure 3. <i>Staphylococcus aureus</i> in Gram's Stain	22
Figure 4. Schematic representation of magnetron sputtering process	28
Figure 5. Schematic representation of a backscatter spectrometry system.....	33
Figure 6. RBS experiment representation.....	34
Figure 7. RBS calibration spectra.....	35
Figure 8. Calibration curve constructed through channel-energy association.....	36
Figure 9. Schematic representation of the contact method.	38
Figure 10. Schematic representation of the contact method with the dilution step....	39
Figure 11. Sample images with 30 second silver deposition.	41
Figure 12. Sample images with 3-minute silver deposition.....	42
Figure 13. Sample images with 10-minute silver deposition.....	43
Figure 14. Sample images with 30-minute silver deposition.....	44
Figure 15. Sample images with 3-minute copper deposition.	45
Figure 16. Sample images with 30-second copper deposition.	46
Figure 17. Sample images with 30-minute copper deposition.	47
Figure 18. Sample images with 10-second copper deposition.	48
Figure 19. Samples with silver coating with time depositions of a) 20 seconds, b) 3 minutes, c) 10 minutes and d) 30 minutes.....	49

Figure 20. Samples with copper coating with time depositions of a) 20 seconds, b) 3 minutes, c) 10 minutes and d) 30 minutes.....	49
Figure 21. RBS spectra of the samples analyzed.....	51
Figure 22. Spectrum of silver coated sample with 30 seconds of deposition (Ag30s) focused on a silver nanoparticle.....	53
Figure 23. Contact method test using <i>S.aureus</i> for samples with silver and copper deposition and for pure glass samples used as control group.....	56
Figure 24. Contact method test with serial dilution of 1:100 using <i>S. aureus</i> for samples with silver deposition of 30 minutes and pure glass samples used as control group.....	59

LIST OF TABLES

Table 1. Papers performed in the last 10 years about Ag-based materials impregnated in woven and non-woven fabrics.....	30
Table 2. Papers performed in the last 10 years about Cu-based materials impregnated in woven and non-woven fabrics.....	30
Table 3. Approximate thickness estimated using simulated data.....	50
Table 4. Silver and copper percentages analyzed by EDS.....	54

LIST OF SYMBOLS AND ABBREVIATIONS

WHO	World Health Organization
EPA	Environmental Protection Agency
PPE	Personal Protective Equipment
PVD	Physical Vapor Deposition
Ag	Silver
Cu	Copper
Au	Gold
Mg	Magnesium
Zn	Zinc
Ti	Titanium
Ar	Argon
Pt	Platinum
H ⁺	Hydrogen Ion
He ⁺	Helium Ion
AgNPs	Silver Nanoparticles
CuNPs	Copper Nanoparticles
RBS	Rutherford Backscattering Spectrometry
SEM	Scanning Electron Microscopy
EDS	Energy Dispersive Spectroscopy
SE	Secondary Electron
ROS	Reactive Oxygen Species
DC	Direct Current
RF	Radiofrequency
MeV	Megaelectron volt
keV	Kiloelectron volt
kV	Kilovolt
mbar	Millibar
W	Watts
mA	Milliampere
μm	Micrometers
nm	Nanometers

mm	Millimeters
cm	Centimeters
m	Meters
h	Hours
μL	Microliters
deg	Degrees
$^{\circ}\text{C}$	Degrees Celsius
ch	Channel
CFU	Colony-Forming Unit
BHI	Brain Heart Infusion
A	Atomic Mass
N_A	Avogadro constant
ρ	Density

RESUMO

DORNELLES DEWES, Adrielle. Caracterização e Avaliação da Atividade Antibacteriana de Revestimentos Finos e Ultrafinos de Ag e de Cu Depositados em Substrato de Vidro via Magnetron Sputtering. Porto Alegre. 2021. Dissertação. Programa de Pós-Graduação em Engenharia e Tecnologia de Materiais, PONTIFÍCIA UNIVERSIDADE CATÓLICA DO RIO GRANDE DO SUL.

Com a atual pandemia da COVID-19, a população mundial e os trabalhadores da área da saúde precisam utilizar equipamentos de proteção individual (EPIs), principalmente proteções faciais, como máscaras faciais e respiradores, para evitar o contágio pelo vírus SARS-CoV-2. Esses itens fazem a filtragem de partículas, porém não apresentam nenhum tipo de mecanismo antimicrobiano, facilitando a contaminação cruzada. Dessa forma, a fim de funcionalizar esses EPIs, estão sendo estudados novos agentes antimicrobianos, como as nanopartículas metálicas, com destaque para a prata (AgNPs) e para o cobre (CuNPs), que possuem efeito antimicrobiano intrínseco. O recobrimento de superfícies utilizando partículas metálicas possibilitaria modificar a superfície de diversos materiais para que apresentassem ações antivirais e antibacterianas. Neste trabalho, então, foi feita a deposição de AgNPs e CuNPs em substrato de vidro utilizando o método *magnetron sputtering*, para avaliar as atividades bactericidas destes materiais. Buscou-se otimizar as condições de deposição e espessura das camadas depositadas quanto a atividade antimicrobiana de modo a facilitar a translação da técnica para outros materiais de uso em EPIs. As amostras foram caracterizadas utilizando as técnicas de Espectrometria de Retroespalhamento Rutherford (RBS) e de Microscopia Eletrônica de Varredura (MEV) a fim de obter informações a respeito da morfologia, composição química e espessura da camada. Além disto, foram realizados estudos biológicos com a bactéria gram-positiva *Staphylococcus aureus* para avaliar a ações antibacteriana dos revestimentos de Ag e de Cu. Com isto, foi possível confirmar a atividade bactericida contra a bactéria *S. aureus*. As amostras com um menor tempo de deposição mostraram efeito antibacteriano tão satisfatório quanto às amostras com tempos de deposição maiores, além de manterem a transparência das amostras.

Palavras-Chaves: Materiais antibacterianos, prata, cobre, superfícies & recobrimentos, engenharia de superfícies.

ABSTRACT

DORNELLES DEWES, Adrielle. Characterization and Evaluation of Antibacterial Activity of Thin and Ultrathin Ag and Cu Coatings Deposited on Glass Substrate via Magnetron Sputtering. Porto Alegre. 2021. Master Thesis. Graduation Program in Materials Engineering and Technology, PONTIFICAL CATHOLIC UNIVERSITY OF RIO GRANDE DO SUL.

With current COVID-19 pandemic, the world population and especially health workers need to use personal protective equipment (PPE), mainly facial protection, such as facial masks and respirators, to prevent contagion by SARS-CoV-2 virus. These items filter particles, however don't present any kind of antimicrobial mechanism, favoring cross-contamination. Thus, in order to functionalize these EPIs, new antimicrobial agents are being studied, such as metallic nanoparticles, especially silver (AgNPs) and copper (CuNPs), which have an intrinsic antimicrobial effect. The coating of surfaces using metallic particles would make it possible to modify the surface of several materials so that they present antiviral and antibacterial actions. In this work, then, the deposition of AgNPs and CuNPs on glass substrate was performed using the magnetron sputtering method, to evaluate the bactericidal activities of these materials. It sought to optimize the deposition conditions and thickness of the deposited layers in terms of antimicrobial activity of the technique to other materials used in PPE. The samples were characterized using Rutherford Backscatter Spectrometry (RBS) and Scanning Electron Microscopy (SEM) techniques in order to obtain information about morphology, chemical composition and layer thickness. In addition, biological studies were performed with the gram-positive bacterium *Staphylococcus aureus* to evaluate the antibacterial actions of Ag and Cu coatings. With this, it was possible to confirm the bactericidal activity against *S. aureus*. The samples with a shorter deposition time showed an antibacterial effect as satisfactory as the samples with longer deposition times, besides these samples keep the transparency of the samples.

Keywords: antibacterial materials, silver, copper, surfaces & coatings, surface engineering.

1. INTRODUCTION

At the end of 2019 it was identified the first cases of the respiratory disease COVID-19, the Coronavirus Disease 2019, caused by SARS-CoV-2 virus and that has become a global health crisis. (DELLA VENTURA *et al.*, 2020; FAUCI *et al.*, 2020) The COVID-19 outbreak – announced as a pandemic situation by the World Health Organization (WHO) – started in Wuhan (China) in December 2019 and the total number of confirmed cases up 09/30/2022 was 614.385.693, with 6.522.600 deaths (HURAIMEL *et al.*, 2020; WORLD HEALTH ORGANIZATION, 2022). This kind of situation is caused by the uncontrolled spread of infectious microorganisms, such bacteria and viruses – that is the case of COVID-19 outbreak.

Thus, to protect healthcare workers and population, authorities required and recommended the use of Personal Protective Equipment (PPE), such as face shield, surgical masks and respirators, such N95, which are very important barriers to decelerate virus transmission. This kind of PPE block or filter microbial particles, but does not inactivate them, favoring cross contamination. Hence, there is an urgent demand for the development of PPEs with antimicrobial action, or to improve those already existing. Research on new bactericidal and virucidal agents and coatings, is a key factor for achieving that goal. (RAI *et al.*, 2014).

In this scenario, metal nanoparticles, such as zinc, copper, silver, gold, titanium, zinc oxide, silver oxide, copper oxide, have been gaining attention due to their antiviral, antibacterial and antifungal characteristics (KHEZERLOU *et al.*, 2018; RAI *et al.*, 2014). Among them, silver nanoparticles (AgNPs) and copper nanoparticles (CuNPs) stand out for presenting intrinsic antimicrobial properties (WEBSTER; SEIL, 2012). These nanomaterials can be produced and deposited by different methods, including via Physical Vapor Deposition (PVD), such as magnetron

sputtering. This is a rapid and scalable technique, which also allow high control of the content of the active elements in a very reproducible manner (IRFAN *et al.*, 2019; TUDOSE *et al.*, 2019).

Although it is well known that silver and copper show microbiocidal activities, there is still room for improving procedures to produce nanocoatings from them that which minimize material consumption and optimize biocidal action (POGGIO *et al.*, 2020). Therefore, the aim of this project was to evaluate the antibacterial action of Ag and Cu coatings deposited via magnetron sputtering on glass samples and to characterize the specimens of interest. The knowledge raised using glass samples will allow a better understanding of metal concentrations or film thickness that optimize antimicrobial activity, paving the way to advance for other substrates, such as synthetic fibers, textiles or face masks.

2. OBJECTIVES

The general aim of this project is to produce and characterize silver and copper coatings deposited on glass substrate via magnetron sputtering and to evaluate their antibacterial properties.

2.1. Specific Objectives

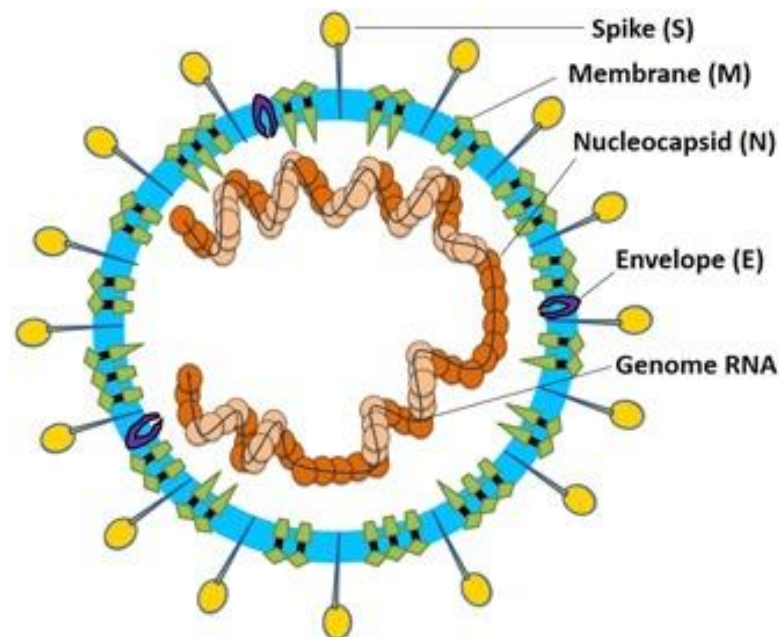
- To produce Ag and Cu coatings via magnetron sputtering on glass substrates and to evaluate the formation of Ag or Cu nanoparticles using magnetron sputtering method.
- To characterize the samples using different techniques, such as Scanning Electron Microscopy (SEM), Energy Dispersive RX Spectroscopy (EDS), and Rutherford Backscattering Spectrometry (RBS), to obtain information about morphology and chemical composition.
- To investigate optimal conditions by which Ag and Cu coatings present antibacterial action against *Staphylococcus aureus*.

3. BACKGROUND

3.1. Viruses and Bacteria

One of the problems we must face in human history is the appearance of new types of viruses and bacteria, a health emergency that can affect people in many ways, mainly when it comes to a pandemic. That is the case of COVID-19, caused by severe acute respiratory syndrome coronavirus 2 (SARS-CoV-2) (HURAIMEL *et al.*, 2020). Viruses are non-cellular pathogens with sizes that varies between 20 to 300nm and depend on a host cell to ensure their viability. This means they need to infect a cell to get energy, cellular machinery – chemical and physical constituents of the cell essential for physiological functions –, and molecular building-blocks for replication. Viruses have genetic material, which can be DNA or RNA, single- or double-stranded, and its genome is coated by a protein shell called capsid. Some viruses have yet an extra protection, a glycoprotein envelope (CARTER; SAUNDERS, 2007; PARKER *et al.*, 2016). SARS-CoV-2 is an example of enveloped virus and it is formed by a single-stranded RNA, a nucleocapsid protein (N), a protective layer associated to a membrane protein (M), to a spike protein (S) and to an envelope protein (E) (WANG *et al.*, 2020). Figure 1 illustrates SARS-CoV-2 virus.

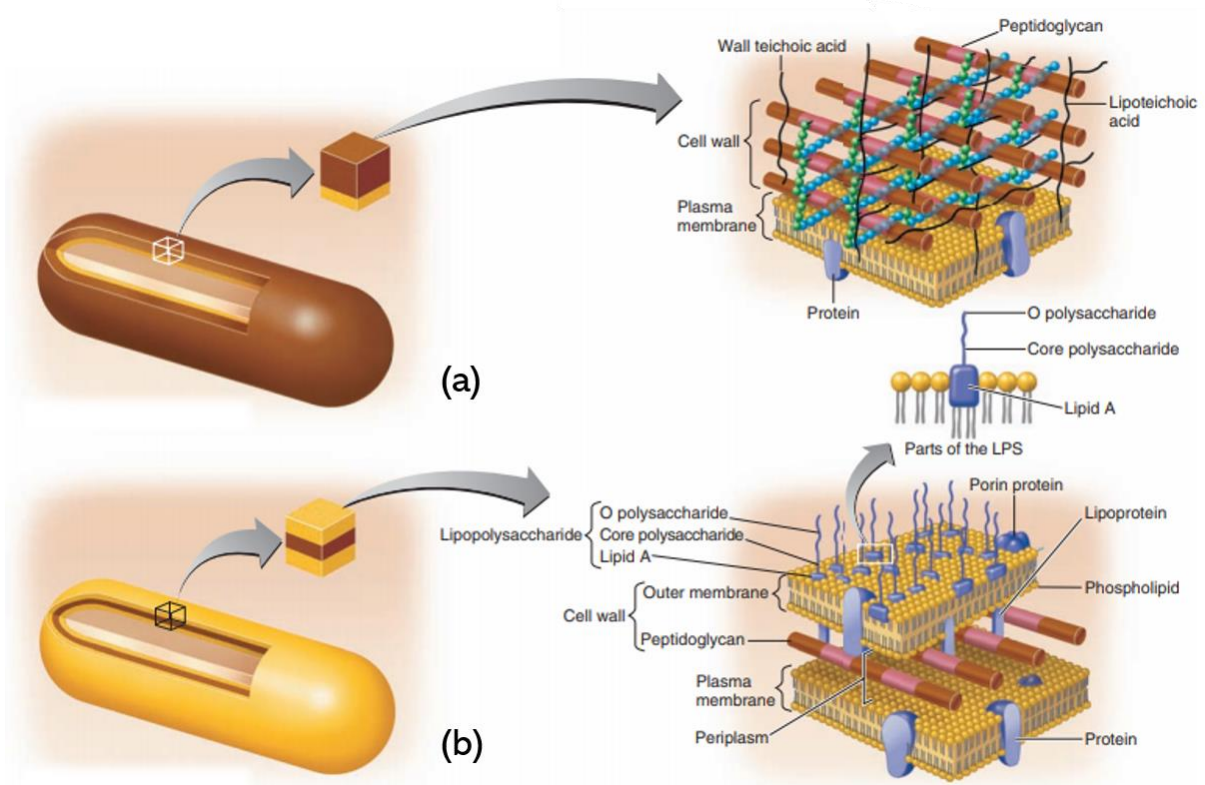
Figure 1. Schematic representation of SARS-CoV-2 structure.



Source: (LI *et al.*, 2020).

In addition to viruses, other microorganisms that can cause outbreaks include bacteria. Bacteria are prokaryotic unicellular organisms. They can have different shapes and sizes, typically found in the form of micrometric spheres or sticks/rods (PARKER *et al.*, 2016; PRESCOTT *et al.*, 2002). The vast majority of bacteria have a cell wall covering the cytoplasmic membrane. They are classified in two types, called gram-positive (e.g., *Staphylococcus aureus*) and gram-negative bacteria (e.g., *Escherichia coli*), according to the Gram Staining method (LEVINSON, 2011, P. 19). In gram-positive bacteria, cell wall is composed by a thick peptideoglycan layer, while in gram-negative there is a thinner peptideoglycan layer and an external membrane. The outer layer of gram-negative bacteria is composed by lipopolysaccharides, lipoproteins and phospholipids (LEVINSON, 2011, P. 18). The differences between the two types are demonstrated in Figure 2.

Figure 2. Representation of cell walls of gram-positive (a) and gram-negative (b) bacteria.



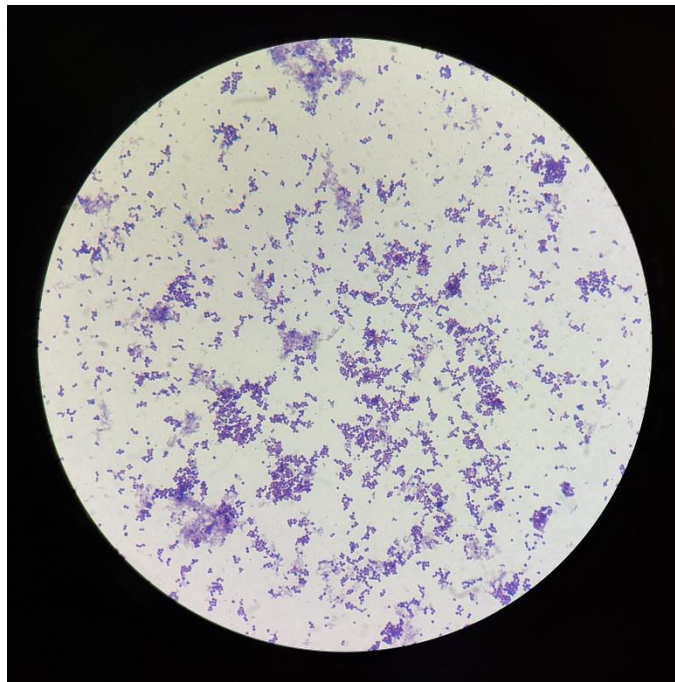
Source: Edited from Tortora, Funke e Case (2013, P. 85).

Therefore, to prevent diseases caused by these microorganisms and their spread, it is important to find new strategies to combat these pathogens which, despite their sizes, can originate serious problems. In this scenario, nanotechnology appears as a very powerful tool, bringing new methods of treatment, diagnostic and prevention (KERRY *et al.*, 2019; SINGH *et al.*, 2017).

In this study it was used *Staphylococcus aureus* to evaluate antibacterial properties of the deposited coatings. *Staphylococcus aureus* is a gram-positive cocci with sizes that varies between 0.5 to 1.5 μm that belongs to Micrococcaceae family. *S. aureus* can cause skin, respiratory, joint, bone, endovascular and soft-tissue disorders, mostly in people with a previous risk factor for infection. This kind of

bacteria appears in clusters with a purple coloration on Gram's Stain. Gram's Stain is a bacterioscopic technique, which in general follows a standardized protocol, widely used in the microbiology laboratories to identify gram positive and gram-negative bacteria and classify their size, shape, cell disposition, and coloration. Gram positive bacteria stain purple and gram negative stain pink. Figure 3 show a microscope image *S. aureus* after Gram's Stain.

Figure 3. *Staphylococcus aureus* in Gram's Stain.



Source: The Author (2021).

3.2. Nanoscience and Nanotechnology

Nanoscience works with structures that present at least one of their physical dimensions below 100nm (MELO; PIMENTA, 2004) (HORNYAK; DUTTA; TIBBALS; RAO, 2008). A nanosized material possesses distinctive properties from those presented by bulk material (RAI et al., 2014). Besides, nanostructures allow a reduction of the energy and mass consumption and high integration and can be structured to present multiple functions in very small spaces. Nanotechnology applies nanoscience to the development of new devices and process that explore the unusual chemical and physical properties of mater at the nanoscale. These

properties are also strongly related to the nanomaterial high surface-to-volume ratio; increasing, e.g., the reactivity of the material (RAI et al., 2014). Nanotechnology is a convergent and multidisciplinary discipline with a wide range of applications (HORNYAK; DUTTA; TIBBALS; RAO, 2008; LIAO; LI; TJONG, 2019). Distinct and independent areas in science link up in the “nano world” and open possibilities of scientific and technological development with potential to change the way we live, by having a huge social impact (HORNYAK; DUTTA; TIBBALS; RAO, 2008).

Investments in nanotechnology have grown exponentially, as it is a very promising area in solving current and future problems. Social implications reach countless fields of interest of society, as environmental, education, economy, and health. However, applying nanoscience in industry and medicine, to develop devices, treatments, and many other technologies is complex. Legislative issues, lack of detailed knowledge of the risks involved in nanotechnology, along with the need to develop cost-effective and reliable methods of manufacture are aspects that hinder the advance of nanotechnology (HORNYAK; DUTTA; TIBBALS; RAO, 2008; MAILLARD; HARTEMANN, 2012).

One of the current challenges nanotechnology is also offering interesting solutions is on the control of pandemics. Pandemic situations brings great socioeconomic impact, and risks to all people, and specially for healthcare workers and high risk groups. (AHMED et al., 2020). Therefore, scientists of different areas have recently worked intensively in the search for new strategies to combat or to avoid outbreaks of diseases caused by viral and bacterial agents. There is a great demand for the development of vaccines, treatments, new diagnostics, materials to improve safety equipment, and other approaches that may help to face this kind of circumstances.

Today, despite all the advances made in the health areas which help to protect the population, when it is necessary to face situations such as the COVID-19 Pandemic, there are still several limitations related to the current methods of prevention (GALDIERO et al., 2011). In this context, nanoscience has been gaining prominence with several studies including the development of nanovaccines, antiviral therapies, theranostics, viral detection and inactivation mechanisms, surface

disinfection technologies, personal protective equipment (PPE) improvement strategies, and other nano-based approaches (LIAO; LI; TJONG, 2019).

3.2.1. Metal Nanoparticles as Biocidal Agents

The small size of nanoparticles allows them to interact with microorganisms, such as viruses and bacteria (RAI *et al.*, 2014). The large surface area permits a precise and direct contact with the microbes' surface and their internal structure (LIAO; LI; TJONG, 2019). Different types of nanoparticles have been studied to combat viruses and bacteria (CAMPOS *et al.*, 2020; KERRY *et al.*, 2019; PATRA *et al.*, 2018; SINGH *et al.*, 2017). Among the huge variety of nanoparticles, metallic nanoparticles stand out as potential agents when it comes to antimicrobial activity (FOUAD, 2021). Metal nanoparticles present a wide antimicrobial spectrum; they can cause a huge damage in the structures of viruses and bacteria (CAMPOS *et al.*, 2020). Some examples are gold (Au), copper (Cu), magnesium (Mg), zinc (Zn), titanium (Ti) and silver (Ag) (KHEZERLOU *et al.*, 2018; RAI *et al.*, 2014).

The mechanism of action of metal nanoparticles is not yet fully established, but there are some possibilities that could explain their antimicrobial activity. First, nanoparticles can induce the production of reactive oxygen species (ROS) on the surface, resulting in oxidative stress on cellular components, including proteins and nucleic acids. This process also can affect viruses too. (CINTEZA *et al.*, 2018) Furthermore, the toxicity of free metal ions released from the surface of the nanoparticle can be high enough to cause irreparable damage on biological structures (KHEZERLOU *et al.*, 2018). Some characteristics of nanoparticles can influence the bactericidal and virucidal effects, such as shape, size, chemical composition, zeta potential, morphological structure, solubility, concentration and even the method of synthesis (EREMENKO *et al.*, 2016; KHEZERLOU *et al.*, 2018; LIAO; LI; TJONG, 2019; SHANKAR; RHIM, 2017; WEBSTER; SEIL, 2012). In summary, metal nanoparticles have proven to be interesting antimicrobial agents, because of their potential to easily bind to fundamental biological elements, such as membranes and genetic material; impairing essential biological functions, as

replication and protein synthesis, and compromising the structural integrity of DNA and RNA (CINTEZA *et al.*, 2018).

3.2.1.1. Silver Nanoparticles (AgNPs)

In the past, silver was used in wounds to aid healing, in the treatment of infections, and to preserve water by storing it in silver-based vessels (KOWALCZYK *et al.*, 2021; MAILLARD; HARTEMANN, 2012). Also, in the second half of the 20th century, silver-based disinfectants began to be used (MAILLARD; HARTEMANN, 2012). Silver is a noble metal that presents an intrinsic antimicrobial effect and inhibitory potential at low concentrations, even in the bulk form, such as zinc (Zn) and copper (Cu) (MAILLARD; HARTEMANN, 2012; WEBSTER; SEIL, 2012). Nevertheless, it is possible to improve the antimicrobial activity, decreasing the particle size because of the increase in surface area. Silver nanoparticles are characterized by exhibiting very good electrical conductivity and chemical stability (LIAO; LI; TJONG, 2019). They are known for its relatively low toxicity to human cells. In spite of that, it is also possible to decrease toxicity and improve the antimicrobial potential of silver nanoparticles using stabilizers (KOWALCZYK *et al.*, 2021; MAILLARD; HARTEMANN, 2012; WEBSTER; SEIL, 2012), such as polymer coatings (MAILLARD; HARTEMANN, 2012).

Silver NPs can exhibit various mechanisms of action against biological agents (WEBSTER; SEIL, 2012). According to studies cited by Maillard and Hartemann (2012), silver nanoparticles present two main pathways of antimicrobial action. One is an intracellular mechanism, and the other is an extracellular mechanism. For the case of bacteria, silver nanoparticles demonstrated bactericidal action for both types of bacteria, gram-positive and gram-negative, including the multidrug resistant (MDR) (LIAO; LI; TJONG, 2019). The antibacterial action of silver nanoparticles is related with their surface charge; positively charged AgNps show more elevated antibacterial activity than the negatively charged and neutral AgNPs (LIAO; LI; TJONG, 2019). AgNPs with sizes less than about 80 nm can interact with the bacterial cell membrane and penetrate through surface proteins (MAILLARD; HARTEMANN, 2012). This process results in modifications in the protein-lipid covering and consequently in cell death (KOWALCZYK *et al.*, 2021). Silver nanoparticles interact with certain compounds that constitute the bacteria cell wall, like thiol groups and with

components containing phosphorus. This interaction cause damages to DNA in consequence of increased permeability – occur when particles with sizes up to 10 nm form pores on the cell wall, causing a leak in the cytoplasm by the entrance of these particles in the cell (LIAO; LI; TJONG, 2019; MAILLARD; HARTEMANN, 2012) –, impaired respiration, and ionic disorders. The protein synthesis is blocked due to the excess of metabolites in the cell (CRUZ *et al.*, 2015; KOWALCZYK *et al.*, 2021; LIAO; LI; TJONG, 2019). Beyond that, silver nanoparticles are capable of generate oxidative stress, destroying DNA through oxidation or alkylation of the bases (KOWALCZYK *et al.*, 2021).

For viruses, when silver nanoparticles present sizes similar to the virus, the antiviral action is manifested by the binding of these nanoparticles with the nucleic acid, damaging the structure of DNA or RNA, and preventing viral replication (KOWALCZYK *et al.*, 2021). Silver nanoparticles can also interact with virus surface proteins, damaging the protective membrane of the virus (MAILLARD; HARTEMANN, 2012). AgNPs interact preferably with proteins rich in sulfhydryl groups and break up disulfide bonds, injuring the protein (JEREMIAH *et al.*, 2020; LARA *et al.*, 2011). For the specific case of the SARS-CoV-2, e.g., disulfide bonds play an essential role in binding the SARS-CoV-2 spike protein (S) to the angiotensin converting enzyme-2 (ACE2) of cells (JEREMIAH *et al.*, 2020). In addition, silver also interacts with different chemical groups like amino, carboxyl, phosphate, and imidazole (LARA *et al.*, 2011). Therefore, the antimicrobial mechanisms of action of silver nanoparticles yet has a lot to investigate, although some possibilities are already documented (KOWALCZYK *et al.*, 2021).

Silver nanoparticles have been incorporated into different materials for microbicidal purposes, such as fibers, coatings, membranes, thin films, gels, fabrics, and liquid solutions (MAILLARD; HARTEMANN, 2012). In textiles applications, e.g., AgNPs prevent bacterial adhesion and growth (LIAO; LI; TJONG, 2019).

3.2.1.2. Copper Nanoparticles (CuNPs)

Copper is also used since antiquity as disinfectant in wounds and to carry water in copper-based vessels (POGGIO *et al.*, 2020). Copper as well as silver is also known for its broad spectrum of antimicrobial action and it is considered cheaper

than AgNPs (EREMENKO *et al.*, 2016; ZOWALATY *et al.*, 2013). However, due to the rapid oxidation of CuNPs when they are exposed to air, to work with them ends up presenting some difficulties and limitations (KHEZERLOU *et al.*, 2018; ZOWALATY *et al.*, 2013). The proposed mechanisms of action for CuNPs are quite similar to the mechanisms of AgNPs (RAFFI *et al.*, 2010). Copper nanoparticles release ions that destroy the bacteria membrane and their cell wall, causing cytoplasm leakage and oxidation of cell components; copper shows a powerful reduction potential that justify the damages caused by these nanomaterials (RAFFI *et al.*, 2010). It is propounded CuNPs have high affinity with elements such as phosphorous and sulfur, for this reason they can interact, e.g., with DNA (RAFFI *et al.*, 2010). Besides, copper nanoparticles showed more affinity with groups like amines and carboxyl than silver nanoparticles, presenting in these cases higher bactericidal effect (EREMENKO *et al.*, 2016). Since copper has several mechanisms of action that happen at the same time, this may prevent microorganisms from developing resistance to CuNPs (RAFFI *et al.*, 2010).

In the case of viruses, one of the mechanisms of action proposed for CuNPs is the production of ROS what induces fragmentation of genetic material and leads to the viral inactivation; the contact of copper nanoparticles with viral capsid causes irreversible damages to the surface proteins and subsequently to the viral genome (POGGIO *et al.*, 2020).

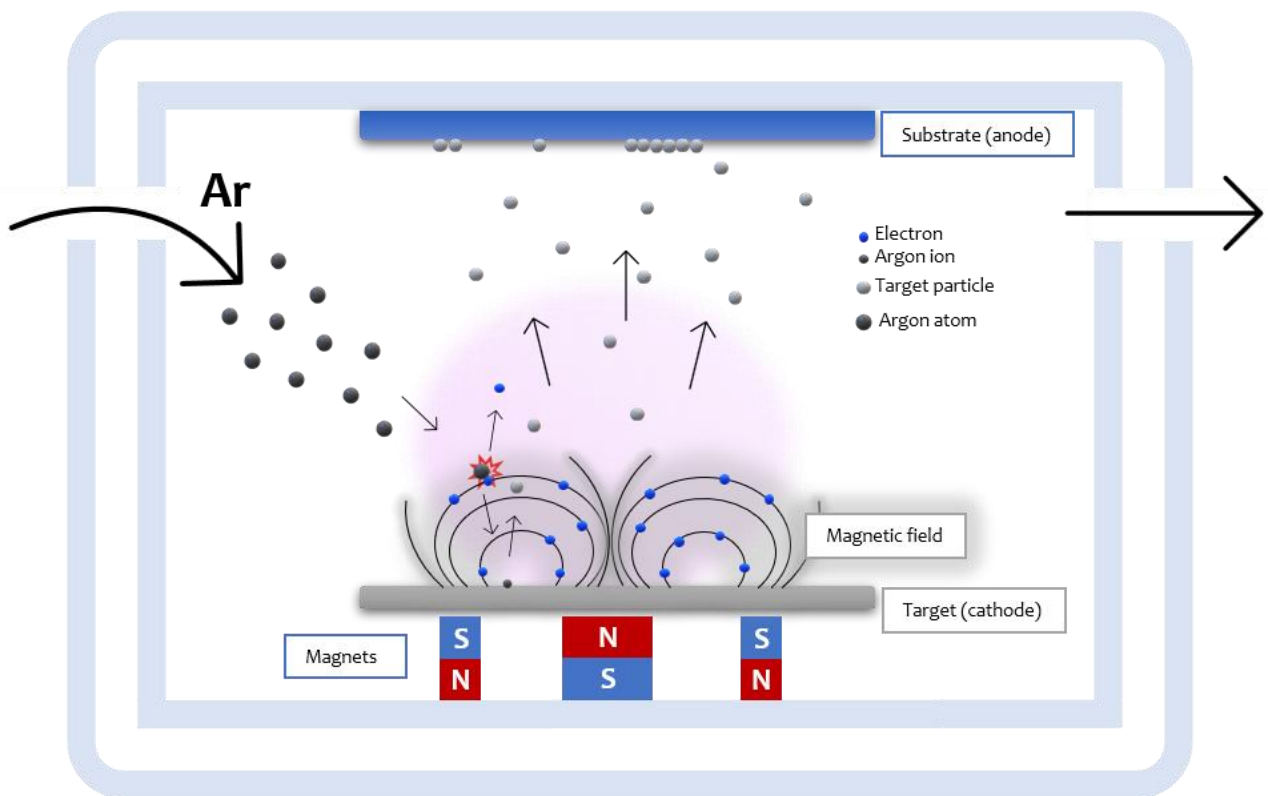
The American Environmental Protection Agency (EPA) consider copper as being the greatest antimicrobial metal and approved several copper alloys to use for different purposes (POGGIO *et al.*, 2020).

3.3. Magnetron Sputtering

Sputtering is a process in which the surface of a material is eroded as a result of ion bombardment, releasing material into the gas phase. When such ejected atoms are collected in a substrate, the process is called sputtering deposition. Magnetron sputtering is a Physical Vapor Deposition (PVD) technique that allows the deposition of high-purity thin films with thickness up to millimeter on a substrate (TUDOSE *et al.*, 2019). Sputtering is a method based on bombarding a target –

anode – by high-energy particles, commonly positive Argon (Ar) ions, to release atoms and molecules from that target onto the substrate of interest – cathode –. The process occurs in a vacuum chamber, where an electric field is produced between two electrodes – the target and the substrate –, and an inert gas is introduced and ionized; resulting in a glow discharge (plasma), sustained by secondary electrons ejected from the target surface (BENETTI *et al.*, 2020; TUDOSE *et al.*, 2019). Magnetron sputtering is a variation of the diode sputtering that uses magnets to generate a magnetic field, where electrons will be imprisoned, increasing the ionization rate (TUDOSE *et al.*, 2019). The process is demonstrated in Figure 4 below.

Figure 4. Schematic representation of the magnetron sputtering process.



Source: The Author (2021).

It is possible with magnetron sputtering to deposit a broad spectrum of materials, including metals, composites, semiconductors and isolators, on various types of substrates – even heat-sensitive substrates – (TUDOSE *et al.*, 2019). It is a

procedure that works with direct current (DC) power, radiofrequency (RF) power, or even pulsed DC power. It is able to perform co-depositions, growing a thin film of more than one kind of material; forming, e.g., alloys (TUDOSE *et al.*, 2019). Furthermore, magnetron sputtering is a dry method characterized by high deposition rates, very good adhesion of films/nanoparticles to the substrate, good coverage of small spaces, and its environmentally friendly nature (no production of chemical waste) (KUDZIN *et al.*, 2020; TUDOSE *et al.*, 2019).

Commercially, magnetron sputtering is a very advantageous technique due to its scalability, being widely used in microelectronics, in decorative coatings, and in the textile industry (IRFAN *et al.*, 2019; TUDOSE *et al.*, 2019). It is interesting using this method for textile applications because it does not damage the fabric fibers neither compromise their bulk properties as a filter element (IRFAN *et al.*, 2019).

3.4. Personal Protective Equipment (PPE)

Thinking about problems that humanity must face, some measures are taken for maintaining the maximum safety of population. The use of Personal Protective Equipment is one of them. Therefore, developing safer equipment to avoid the contamination by viruses or bacteria is essential. Many of these PPE are made of polymeric materials, hence the functionalization of fabrics and non-woven fabrics are also to increase the safety of gloves, foot and eye protection, face masks, respirators and face shields (SPORTELLI *et al.*, 2020).

3.5. State of Art

Table 1 shows a selection of papers on the antimicrobial action of silver nanoparticles and other silver-based materials incorporated into fabrics, nonwoven fabrics, and respirators, using sputtering technique, in the last 10 years. Table 2 exhibit a similar collection of articles, but dealing with antimicrobial action of copper nanoparticles and other copper-based materials.

Table 1. Selection of papers performed in the last 10 years about Ag-based materials.

AUTHORS	JUNG ET AL., 2021	KUDZIN ET AL., 2020	KUDZIN ET AL., 2020	SUBRAMANIAN ET AL., 2014
OBJECTIVES	To develop a copper-coated Korean filter 94 (KF94) masks that present antiviral action against SARS-CoV-2 virus	To prepare and to characterize a multifunctional, biodegradable composite material with antimicrobial action	To fabricate a multifunctional and antimicrobial composite material	To evaluate antibacterial properties of CuO deposited on fabric substrate
ANTIMICROBIAL MATERIAL SYNTHESIS/ INCORPORATION METHOD	Cu	Cu	Cu	CuO
SUBSTRATE	DC magnetron sputtering	DC magnetron sputtering	DC magnetron sputtering	DC magnetron sputtering
MICROORGANISM	Polypropylene (PP) filter	Poly lactide (PLA) non-woven	Polyethylene terephthalate (PET) knitted fabric	Woven and non-woven fabric
	SARS-CoV-2	S. aureus, E. coli and Chaetomium globosum	S. aureus, E. coli and Chaetomium globosum	E. coli and S. aureus

Table 2. Selection of papers performed in the last 10 years about Cu-based materials.

AUTHORS	BALAGNA ET AL., 2020	IRFAN ET AL., 2019	LIU ET AL., 2019	CHUANG ET AL., 2017	SHAHIDI ET AL., 2015	MEI ET AL., 2014	BAGHRICHE ET AL., 2012
OBJECTIVES	To evaluate the antiviral effect for Coronavirus SARS-CoV-2 of a silver nanocluster/silica composite coating	To characterize antibacterial, hydrophobic, and semitransparent metal/plasma properties of a polymer nanocomposite coating	To develop wound dressings with cotton nonwovens impregnated with silver, zinc, and Ag/Zn	To evaluate bactericidal effect of a ZnO/Ag ₂ O composite thin film deposited on non-woven fabric	To create antibacterial and ultraviolet protective cotton fabrics	To functionalize polyamide fabrics with AgNPs to obtain antibacterial activity	To functionalize polyester fibers with AgNPs to be effective in bacterial inactivation
ANTIMICROBIAL MATERIAL	nanocluster/silica-based coating	Ag	Ag and Zn	ZnO/Ag ₂ O composite	Ag	Ag	Ag
SYNTHESIS/ INCORPORATION METHOD	RF/DC magnetron sputtering (co-deposition)	Magnetron sputtering (co-deposition)	RF/DC magnetron sputtering	RF magnetron sputtering	DC magnetron sputtering	DC magnetron sputtering	DC magnetron sputtering and pulsed DC magnetron sputtering (DCP)
SUBSTRATE	Facial FFP3 mask (3MTM)	Cotton fabric	Cotton non-woven	Non-woven fabric	Cotton fabric	Polyamide fabric	Polyester fabric
MICROORGANISM	SARS-CoV-2	Staphylococcus epidermidis	E. coli and S. aureus	S. aureus and E. coli	S. aureus and E. coli	E. coli	E. coli

In addition, other three papers performed studies with silver and copper jointly. MENG *et al.* (2020) used co-deposition via magnetron sputtering technique to impregnate Ag and Cu nanoparticles in polyester fabric; the authors evaluated the structure and properties of an Ag/Cu nanocomposite film. EREMENKO *et al.* (2016)

incorporated silver and bimetallic Ag/Cu NPs in cotton fabric by aqueous solutions of silver and copper salts. Both papers worked with alloys of Ag/Cu, however there is a difference in the technique used and in the properties analyzed. MENG *et al.* (2020) did not aim to investigate antimicrobial properties. EREMENKO *et al.* (2016) evaluated bactericidal and fungicidal activities, although using a chemical route technique. In addition to these two papers, the work of MEISTER *et al.* (2022) also co-deposited Ag and Cu using magnetron sputtering technique to produce a film on the Si substrate. They aimed to analyze the antiviral and antibacterial activities of Ag, Cu, Cu & Ag co-deposited, Ag & Pt co-deposited, Cu on Ag sequentially deposited and Ag on Pt sequentially deposited films.

4. MATERIALS E METHODS

The experimental work of Ag and Cu deposition was conducted at the Centro Interdisciplinar de Nanociência e Micro-Nanotecnologia (NanoPUCRS) and the biological assays in the Laboratory of Immunology and Microbiology at PUCRS. Below, a detailed description of the materials and methods used is given.

4.1. Substrates

As substrate for the deposition of the metals, glass slides with an approximate thickness of 1.0 to 1.2mm cut into 1x1cm squares from Precision Glass Line were used. The samples were sanitized with Extran soap, Milli-Q water and 70% ethyl alcohol before the deposition.

4.2. Metallic Deposition

The deposition of silver and copper metals on the glass was performed using a home-built magnetron sputtering system from the Centro Interdisciplinar de Nanociência e Micro-Nanotecnologia (NanoPUCRS).

A silver and a copper target from Kurt J. Lesker with a purity of 99.9% from Kurt J. Lesker were used. The base pressure reached in the vacuum chamber was 10^{-5} mbar. The working pressure was maintained at 10^{-3} mbar. The base pressure is that reached before deposition. The working pressure is the pressure inside the chamber during the deposition process of the metals. Both pressures are important parameters that are directly linked to the quality of the film. For both materials the deposition power was 50W with an electric current of approximately 134 mA. The samples were produced in four different deposition times for each type of metal (Ag and Cu): 30 seconds, 3 minutes, 10 minutes, and 30 minutes.

Different quantities of silver and copper were deposited, and these quantities were estimated by the time of deposition. All samples were produced in triplicate in order to evaluate the reproducibility of the physical deposition process.

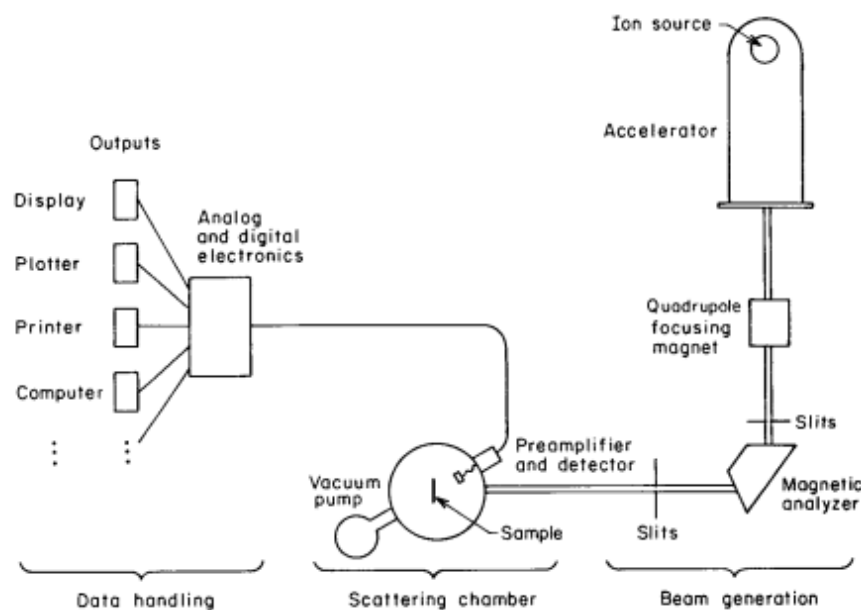
4.3. Characterization Techniques

The characterization of the deposited materials was performed based on two techniques: Rutherford Backscattering Spectrometry (RBS) and Scanning Electron Microscopy (SEM). Biological tests were also carried out for antimicrobial evaluation with the gram-positive bacteria *Staphylococcus aureus*.

4.3.1. Rutherford Backscattering Spectrometry (RBS)

Rutherford backscattering spectrometry (RBS) was used to determine the elemental composition of the samples. Rutherford backscattering spectrometry is a method of characterization based on the scattering of a monoenergetic particle beam (normally H^+ , He^+ , He^{2+}) with energy in the MeV-range, by the atoms of the sample. The technique measures the energy of the backscattered ions using a solid-state detector. Since this energy depends on the Z of the scattering atom, the elements present in the sample can be identified and their depth profile determined. RBS provide quantitative information on the elemental composition of a sample (MAYER, 2003; WITTKÄMPER *et al.*, 2019). A scheme of a RBS system is shown in Figure 5.

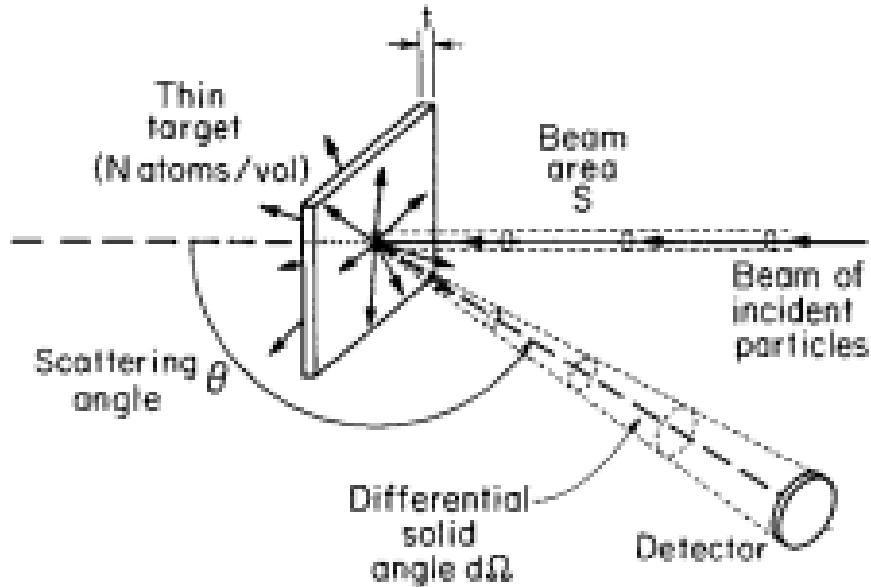
Figure 5. Schematic representation of a Rutherford backscattering spectrometer system.



Source: Chu *et al.* (1978, P. 4).

Figure 6 shows the geometry of a typical RBS experiment.

Figure 6. RBS experiment representation.

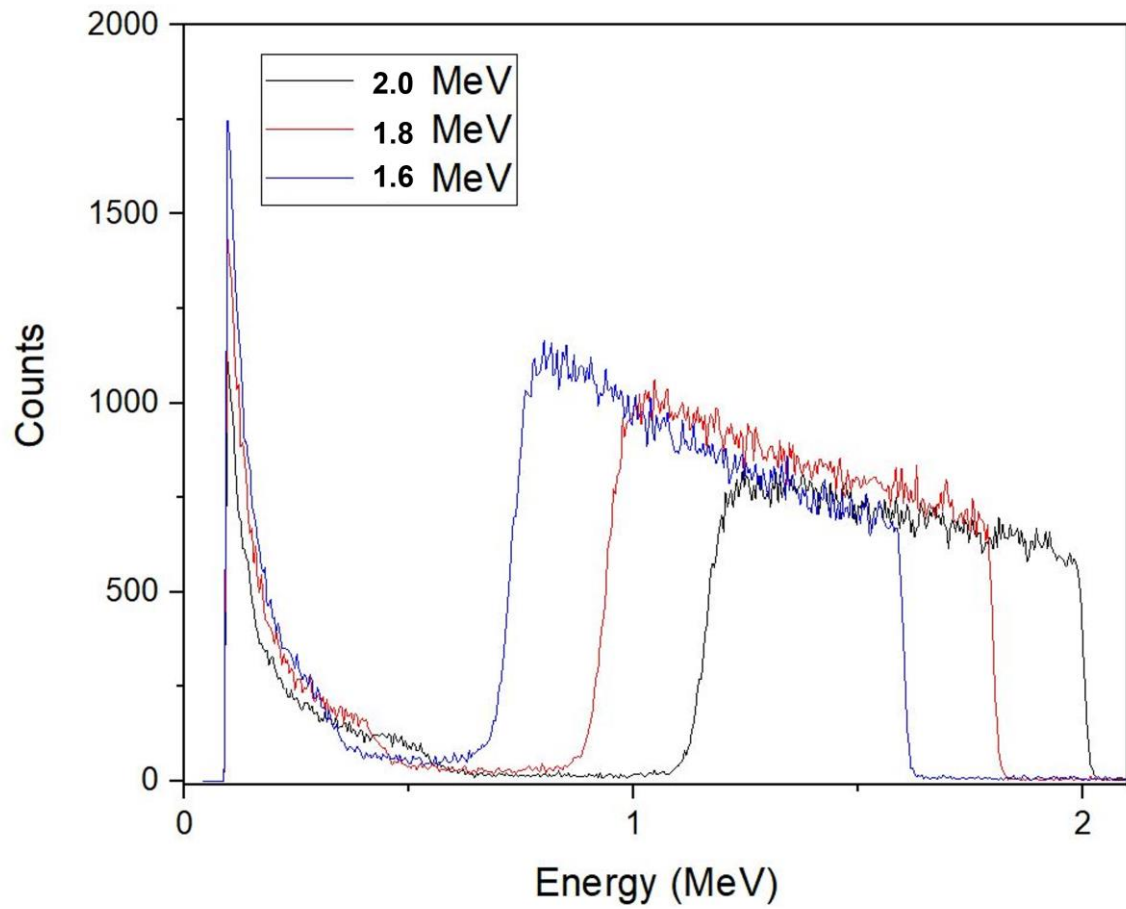


Source: Chu *et al.* (1978, P. 26).

The equipment used to perform the Rutherford backscatter spectrometry measurements belongs to the Laboratório de Implantação Iônica of the Instituto de Física of Universidade Federal do Rio Grande do Sul (UFRGS). The accelerator model is a 3MV 4130HC TANDEM accelerator. RBS measurements were performed using a beam of 2MeV $^4\text{He}^{2+}$ at an incident angle of 0° with the sample normal. Backscattered ions at 165° were detected with a silicon detector (15 keV resolution). Samples for RBS were prepared with the same deposition times, but on a silicon substrate.

Before starting the measurements, a calibration of the detector was performed using a $1\mu\text{m}$ -thick gold (Au) film and four different beam energies: 1.6, 1.8 and 2.0 MeV. In this way, a curve correlating channel number of the energy analyser versus the energy of the beam can be built. Figure 7 shows a typical RBS spectrum used in the calibration and Figure 8 the resulting calibration curve.

Figure 7. RBS calibration spectra.

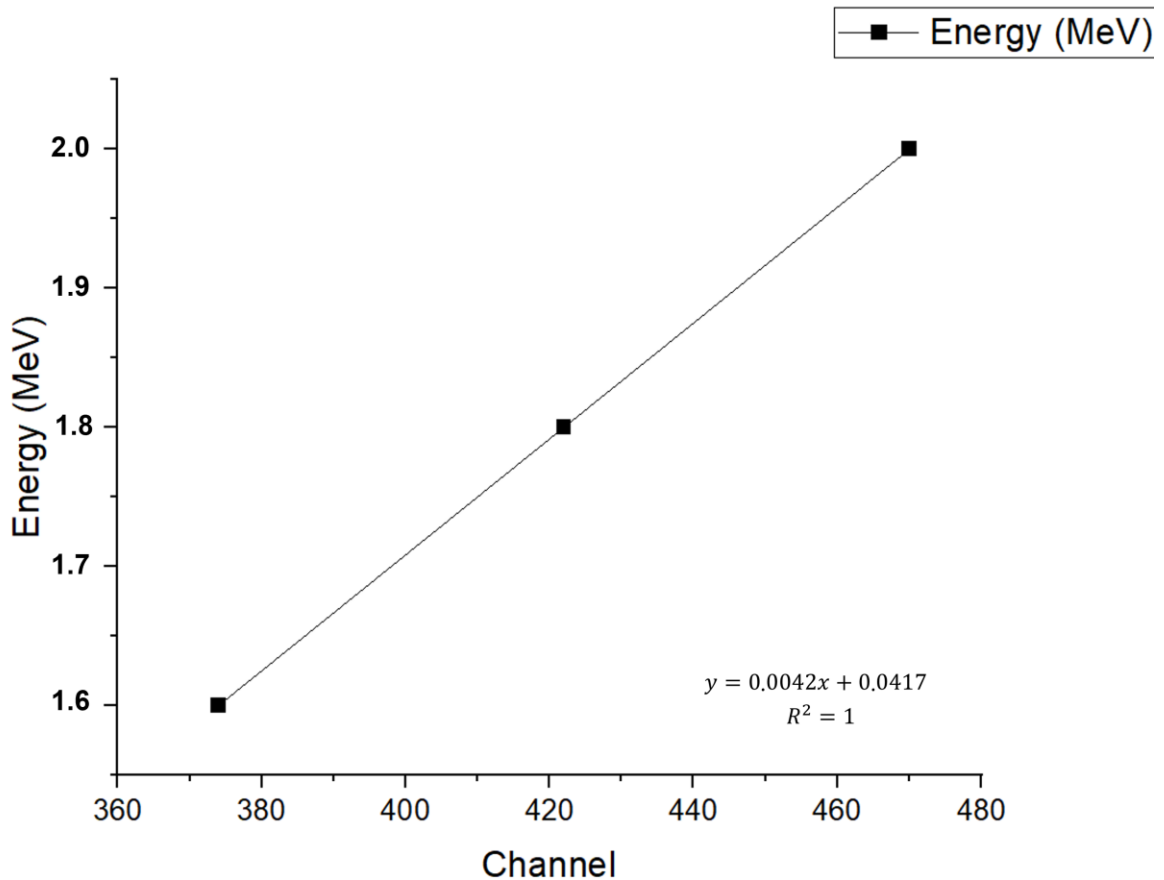


Source: The Author (2021).

For this specific data, the equation of channel number versus beam energy of the scattered beam is:

$$E = (0.0042 * channel) + 0.0417 \quad (2)$$

Figure 8. Calibration curve constructed through channel-energy association.



Source: The Author (2022).

SIMNRA software was also used to simulate the spectra. Input parameters for the program are the incident angle (deg), scattering angle (deg), energy per channel (keV/ch), and the ion beam energy (keV). Besides some sample information is also necessary such as number and thickness of layers and sample composition. After obtaining the RBS spectra, graphs containing the experimental and simulated data were generated using OringLab software.

4.3.2. Scanning Electron Microscopy (SEM)

This technique was chosen to evaluate the qualitative composition and the surface structure of the samples. Scanning electron microscopy generate images from scanning the sample surface using a focused electron beam with high energy,

and what is detected are the backscattered electrons (chemical composition) or the secondary electrons (topographic contrast) (KHARE *et al.*, 2019).

The analysis by SEM was performed at the Laboratório Central de Microscopia e Microanálise (LabCEMM) at PUCRS. The microscope model used was a FEI Inspect F50 operated in the secondary electron mode (SE). Energy Dispersive Spectroscopy (EDS) data was also acquired for qualitative information of material composition. Images were registered with magnifications of 500, 1000, 2000, 5000, 10000 and 20000 times with an acceleration voltage of 20.0 kV.

4.4. Antibacterial Evaluation

The antibacterial test were performed at the Laboratório de Imunologia e Microbiologia at PUCRS with the gram-positive bacteria *Staphylococcus aureus*.

4.4.1. Contact Method

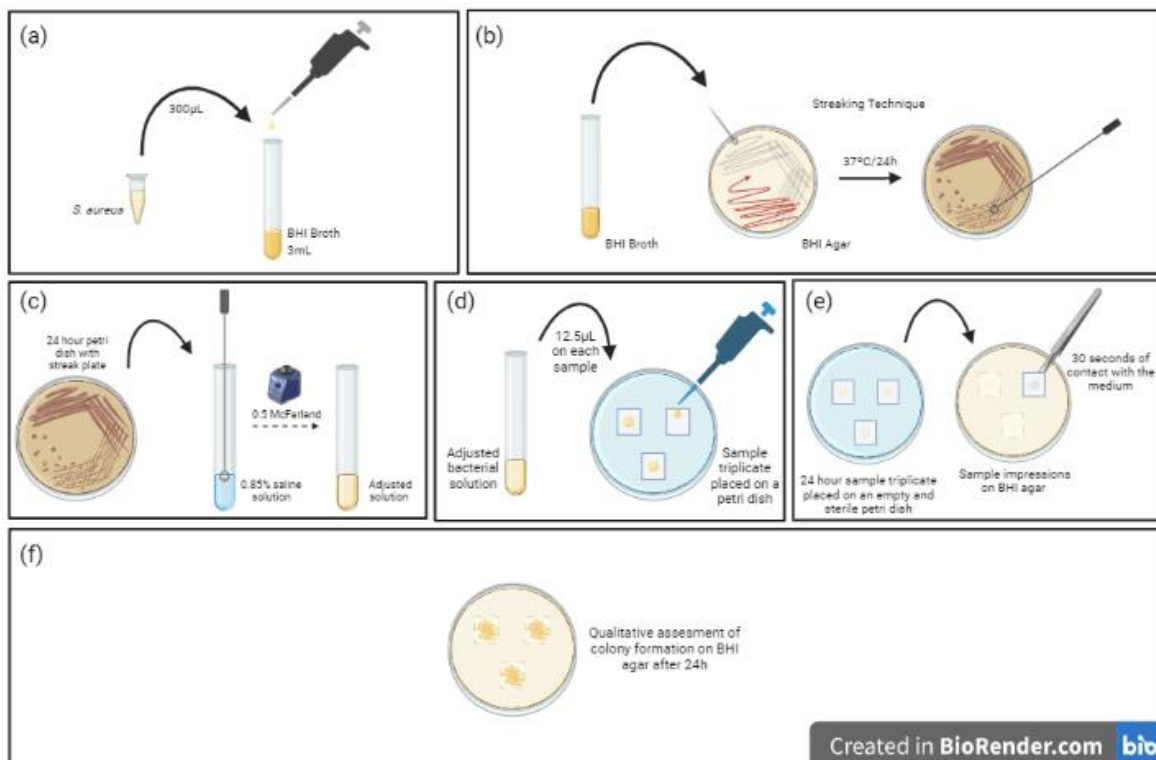
The antimicrobial evaluation was performed using a modified contact method against gram positive bacteria *Staphylococcus aureus* ATCC29213. This method was used as a qualitative approach to evaluate the antibacterial action of Ag and Cu coatings.

First all materials used in the experiment were properly autoclaved for 15 minutes at 121°C in order to guarantee their sterility. The *S. aureus* was cultivated in BHI broth at 37°C for 24h (Figure 9 (a)). A Gram stain test from the 24h broth was done to confirm there was no contamination. The streaking technique was applied mixing an aliquot of the broth in BHI agar in a petri dish, which was also maintained at 37°C for 24h (Figure 9 (b)). The colonies were inoculated in 0.85% saline solution to adjust the bacterial suspension to 0.5 McFarland standard (approximately 10^8 CFU/ml) (Figure 9 (c)). The 1x1cm glass samples were placed at empty and sterile petri dishes and 12.5µL from the adjusted bacterial solution was pipetted on each sample (Figure 9 (d)). The samples with the bacteria on the surface were kept at a temperature of

37°C. After 24h each glass sample was impressed on BHI agar, through the contact of the contaminated surface with the growth medium for 30 seconds (Figure 9 (e)). The plates with the impressions were incubated for 24h. Posteriorly, the results of colony formation or absence of growth were observed (Figure 9 (f)). A total of 27 samples were analyzed, all listed below:

- 3 samples with 30 seconds of silver deposition.
- 3 samples with 30 seconds of copper deposition.
- 3 samples with 3 minutes of silver deposition.
- 3 samples with 3 minutes of copper deposition.
- 3 samples with 10 minutes of silver deposition.
- 3 samples with 10 minutes of copper deposition.
- 3 samples with 30 minutes of silver deposition.
- 3 samples with 30 minutes of copper deposition.
- 3 uncoated samples used as control group.

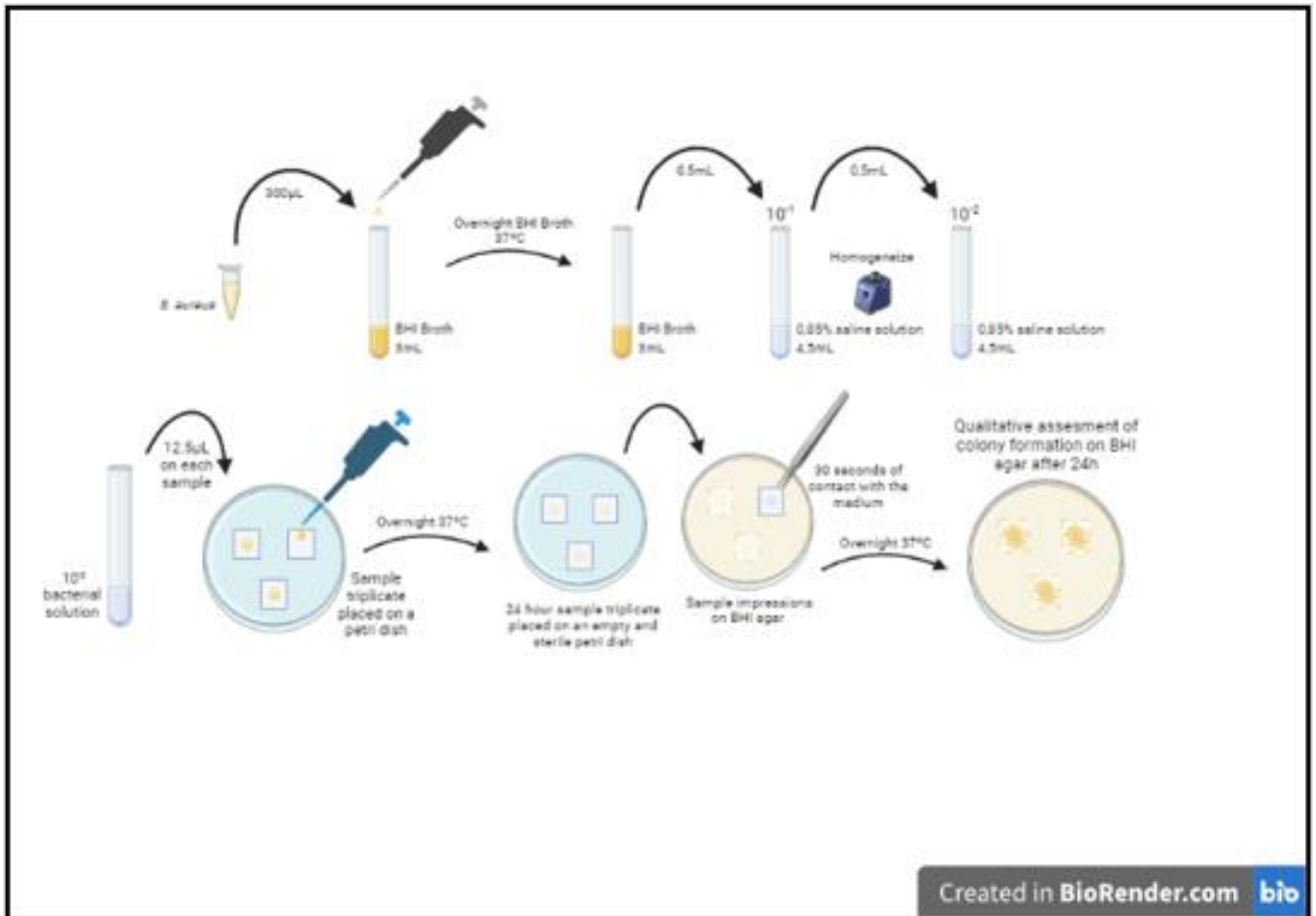
Figure 9. Schematic representation of the contact method.



Source: The Author (2022).

A second test was carried out to repeat the set of samples of 30 minutes silver deposition in order to try performing the counting of colonies. The same contact method was applied but a serial dilution was done before the sample drip step. Figure 10 represent the contact method test with the dilution of 1:100.

Figure 10. Schematic representation of the contact method with the dilution step.



Source: The Author (2022).

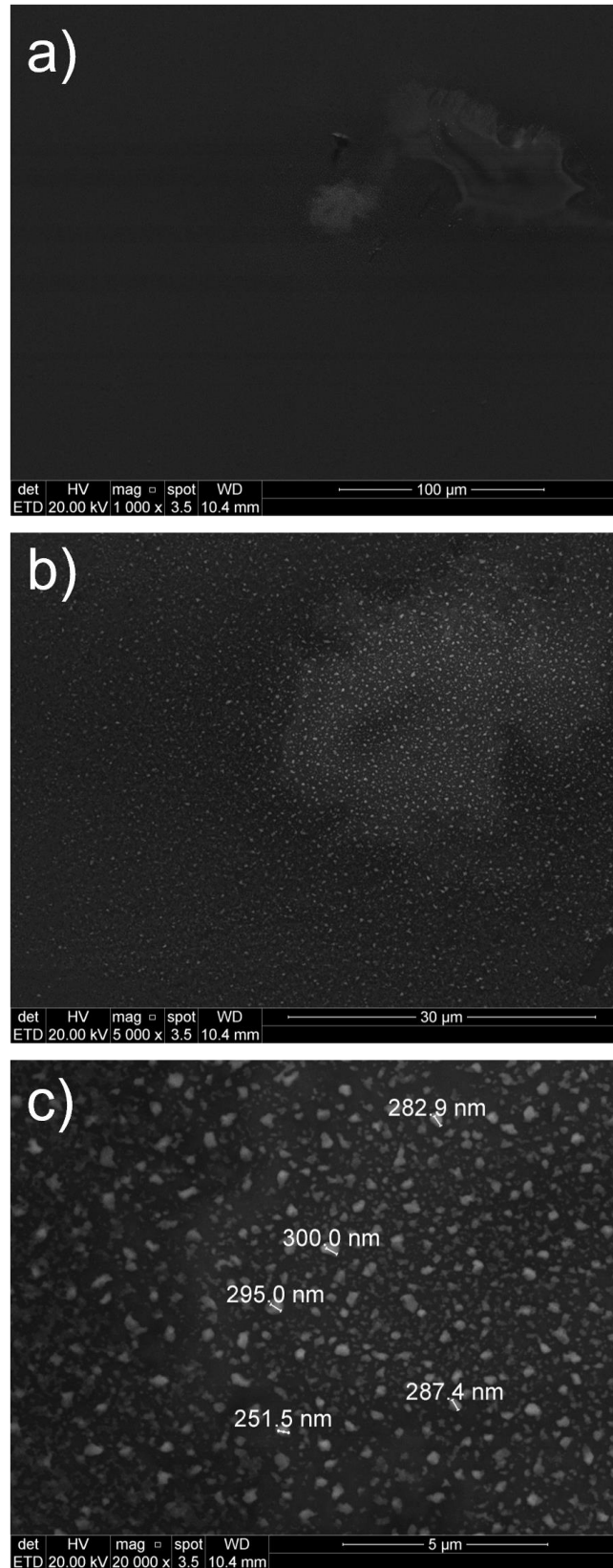
5. RESULTS AND DISCUSSION

5.1. SEM Analysis

Analyzes via Scanning Electron Microscopy were performed in order to observe the morphology of the films produced. Figure 12 shows images obtained by SEM of the samples coated with silver for 30 seconds. For all SEM images represented in Figures 11, 12, 13, 14, 15, 16, 17 and 18, the letters a, b and c correspond to magnifications of 1000, 5000 and 20000 times, respectively. The images of figure 11 show that for the 30s deposition, silver is not distributed uniformly and a film it is not formed. In this case it is possible to notice the formation of clusters and nanoparticles on the glass. Particles have sizes of approximately 200 to 300 nm.

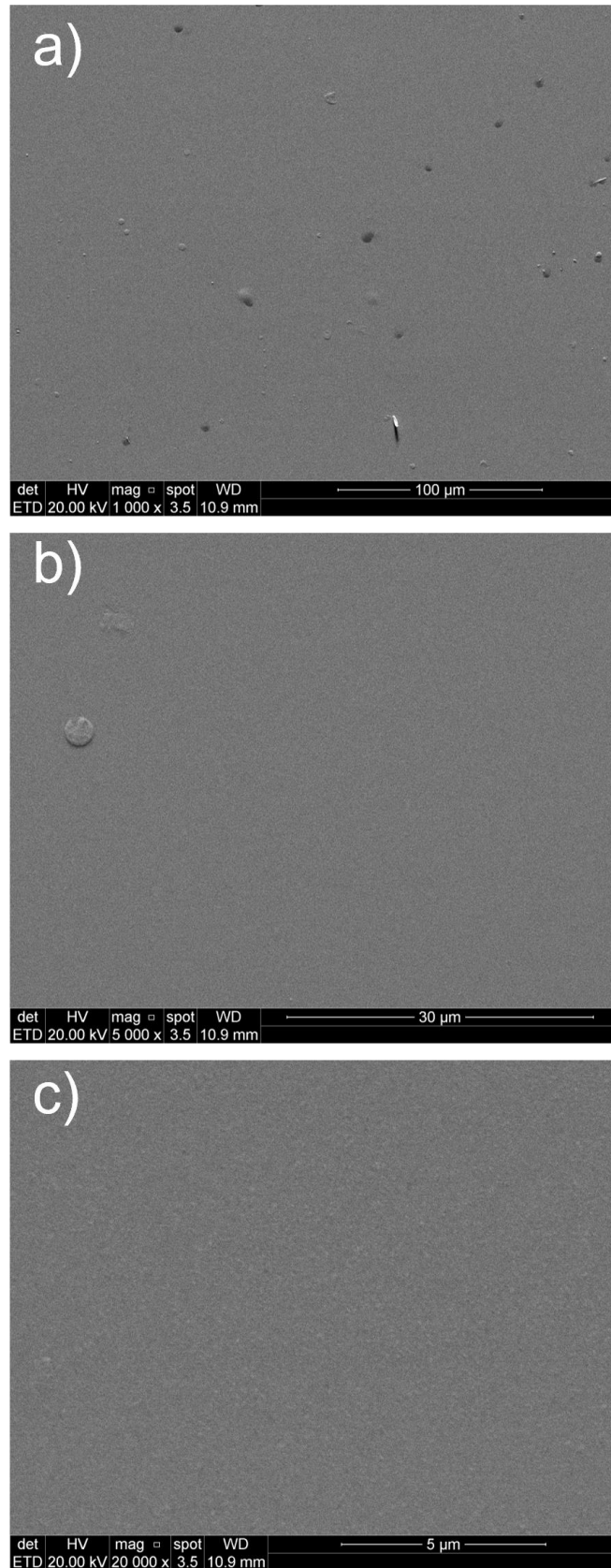
The images of figure 12 shows a thin film formation. There is continuity in the distribution of particles on the glass surface for the deposition time of 3 minutes of silver. It is not observed cluster formation or isolated particles. In figure 12c it is possible to notice the roughness of the surface, possibly from the substrate itself. These rough regions could also represent areas that there was a higher concentration of particles in the deposition process.

Figure 11. Sample images with 30 second silver deposition.



Source: LabCEMM - PUCRS (2022).

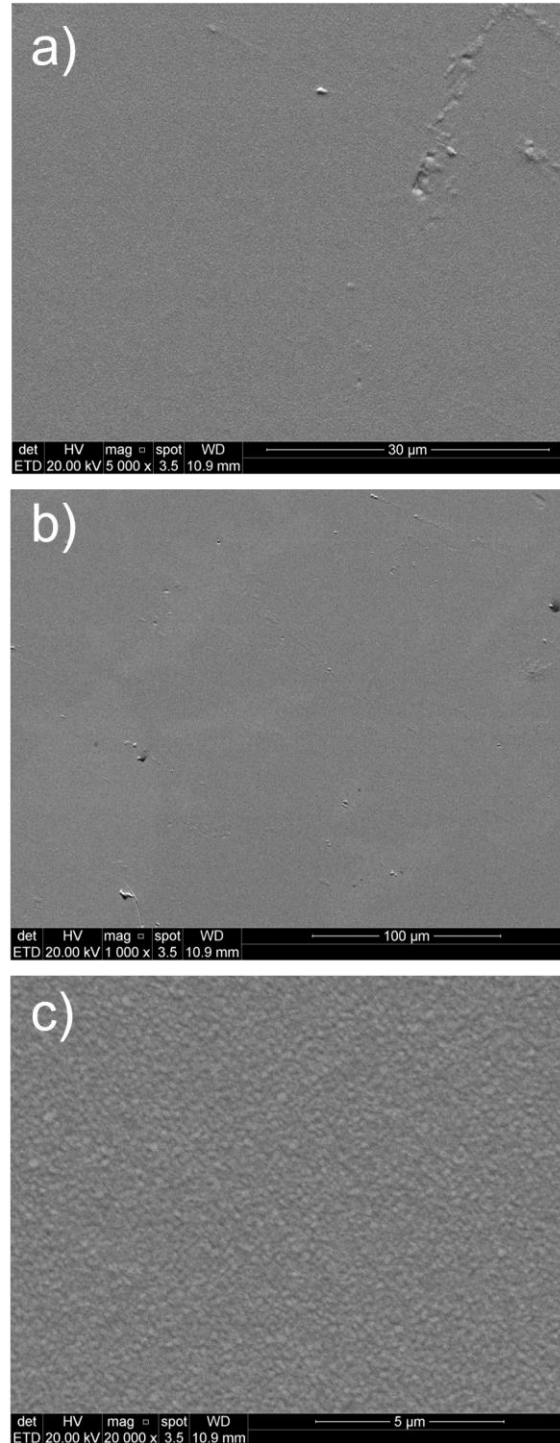
Figure 12. Sample images with 3-minute silver deposition.



Source: LabCEMM - PUCRS (2022).

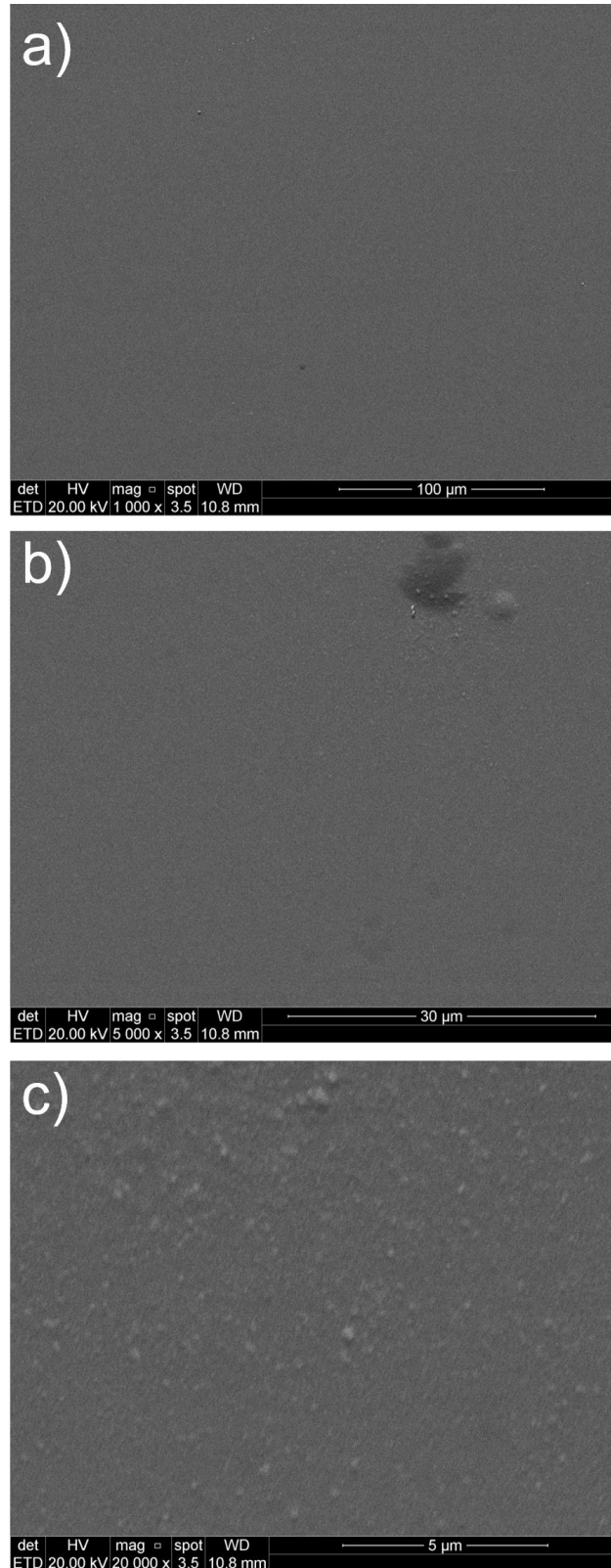
Figures 13 and 14 represent the depositions performed with 10 minutes and 30 minutes of silver, respectively. It is possible to observe a smoother surface than in the shorter time deposition. There are some imperfections on the surface that possibly represents some impurity that remained on the substrate before deposition.

Figure 13. Sample images with 10-minute silver deposition.



Source: LabCEMM - PUCRS (2022).

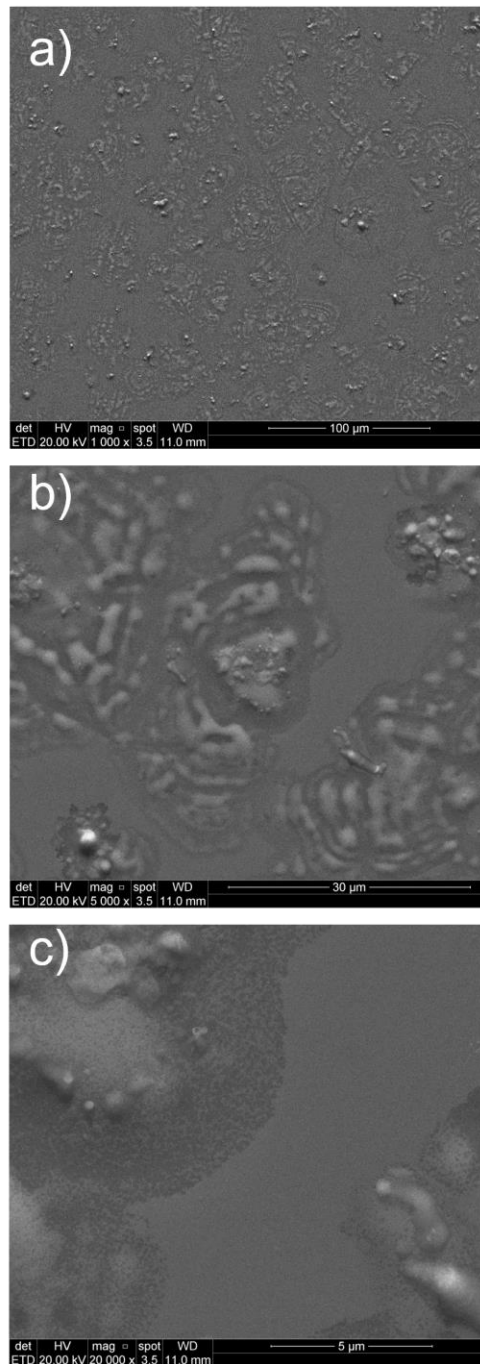
Figure 14. Sample images with 30-minute silver deposition.



Source: LabCEMM - PUCRS (2022).

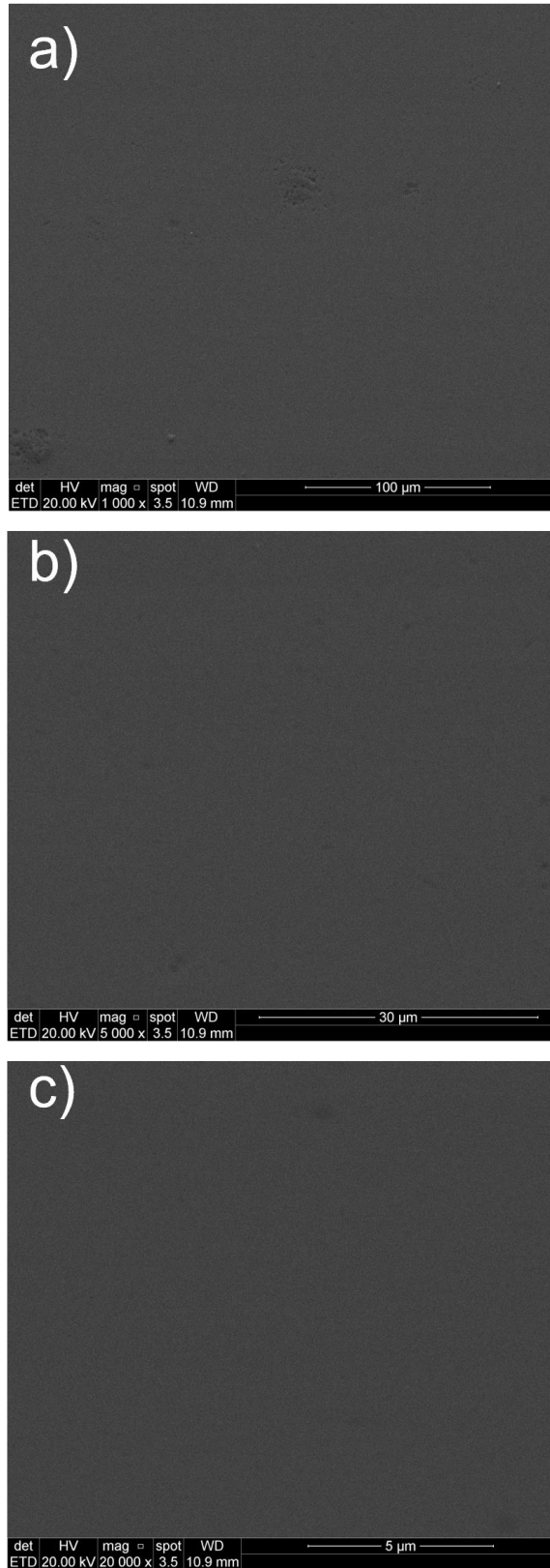
In Figure 15 the images show some marks on the surface what appears to be a bubble formation in the thin film of the samples with 3 minutes of copper deposition. These bubbles are not seen without the aid of the microscope. While in Figure 16 it is possible to observe a smoother and more uniform surface. For longer deposition times the glass surfaces with the film are quite smooth with only a few deformities, as shown in Figures 17 and 18.

Figure 15. Sample images with 3-minute copper deposition



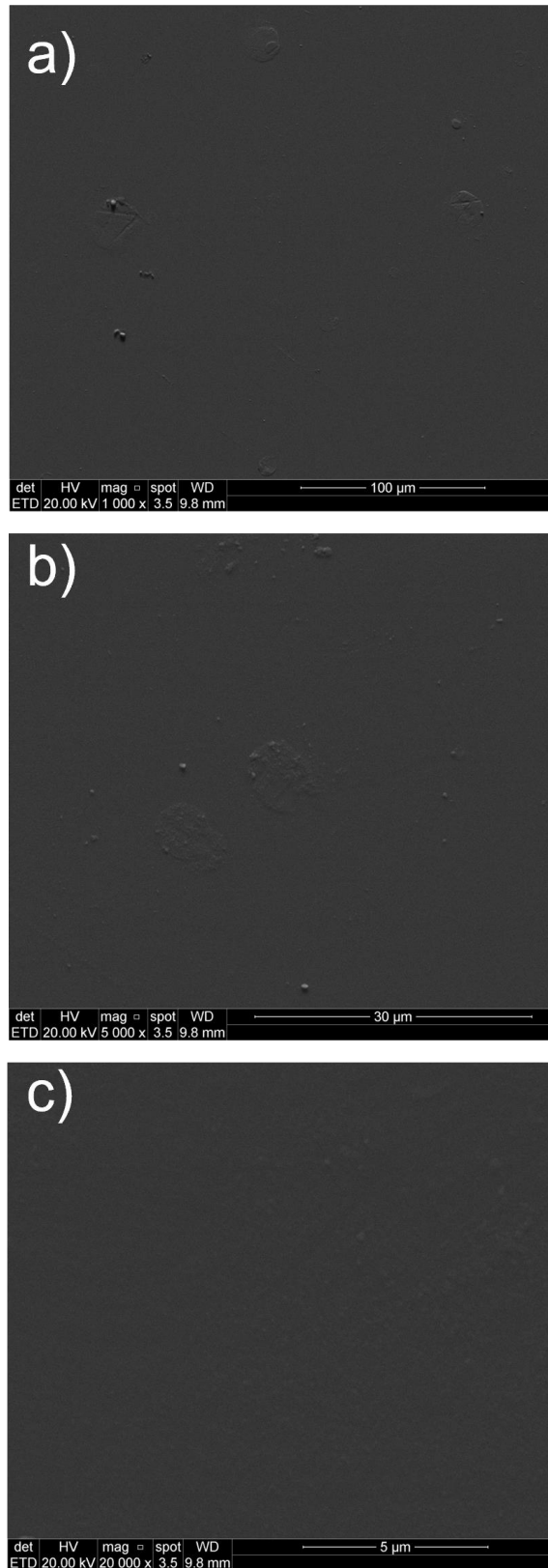
Source: LabCEMM - PUCRS (2022).

Figure 16. Sample images with 30-second copper deposition.



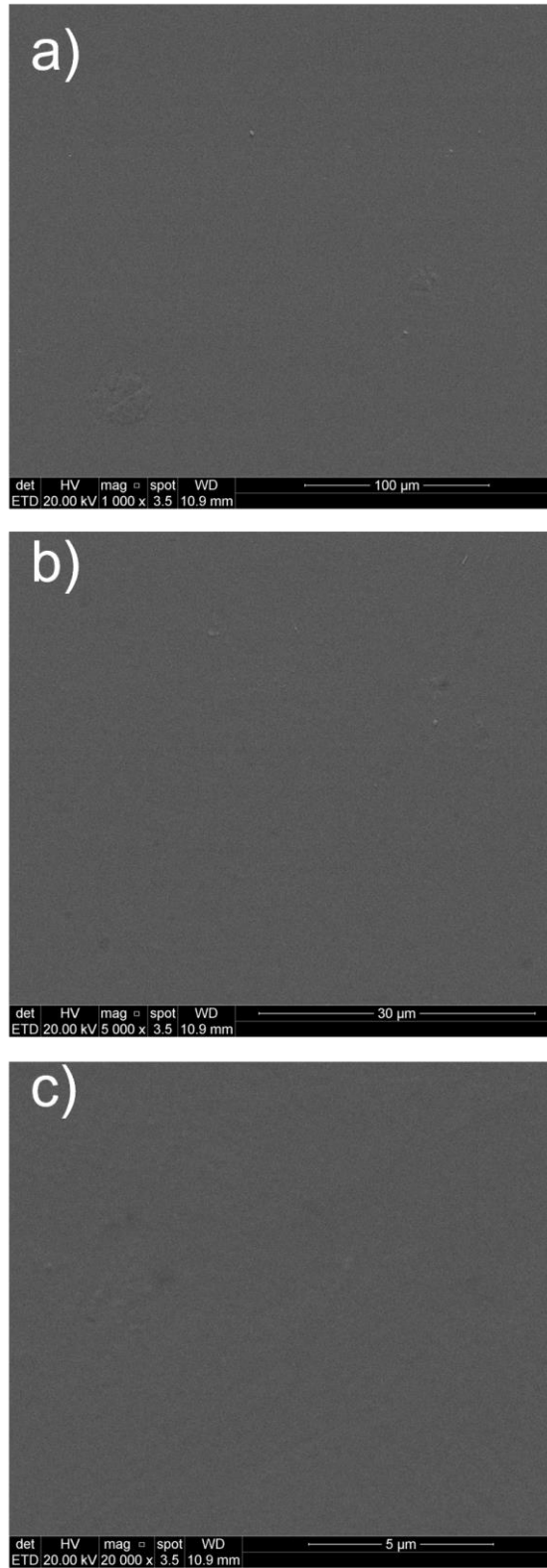
Source: LabCEMM - PUCRS (2022).

Figure 17. Sample images with 30-minute copper deposition.



Source: LabCEMM - PUCRS (2022).

Figure 18. Sample images with 10-minute copper deposition.

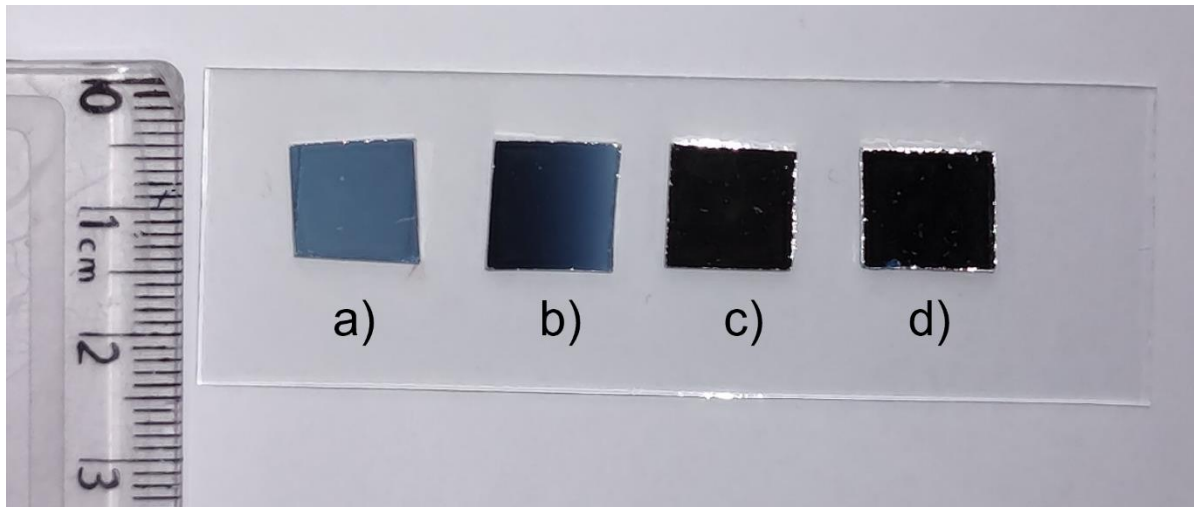


Source: LabCEMM - PUCRS (2022).

5.2. Analysis of the Presence of Silver and Copper on the Samples

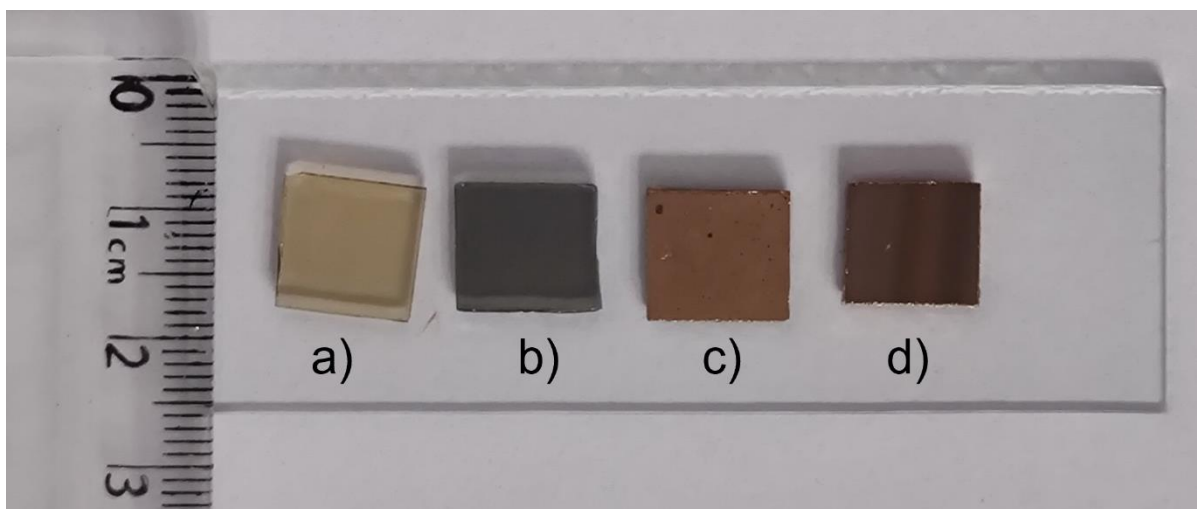
The analysis of silver and copper coatings was done also through Rutherford Backscattering Spectroscopy (RBS) and Energy Dispersive Spectroscopy (EDS). Figure 19 and 20 shows the samples with different concentrations of each metal and different film thickness.

Figure 19. Samples with silver coating with time depositions of a) 30 seconds, b) 3 minutes, c) 10 minutes and d) 30 minutes.



Source: The Author (2022).

Figure 20. Samples with copper coating with time depositions of a) 30 seconds, b) 3 minutes, c) 10 minutes and d) 30 minutes.



Source: The Author (2022).

In Figures 19 and 20 are possible to notice that as the deposition time varies, there is a modification in the color of the film. Besides, the glass substrate without the metallic coating is characteristically transparent. Therefore, it is possible to observe that after the deposition of silver and copper, the glass loses partially or completely its transparency. The thickness of each film was estimated using the equation:

$$thickness = \frac{(atoms\ per\ cm^2) * A}{N_A * \rho} \quad (3)$$

Where A is the atomic mass of the element, N_A is the Avogadro constant, ρ represents the density of the deposited material, and the information of atoms per square centimeter is a value obtained from the simulated RBS spectra carried out on SIMNRA software. The values of the estimated thickness for each sample can be visualized on Table 3 below.

Table 3. Approximate thickness estimated using simulated data.

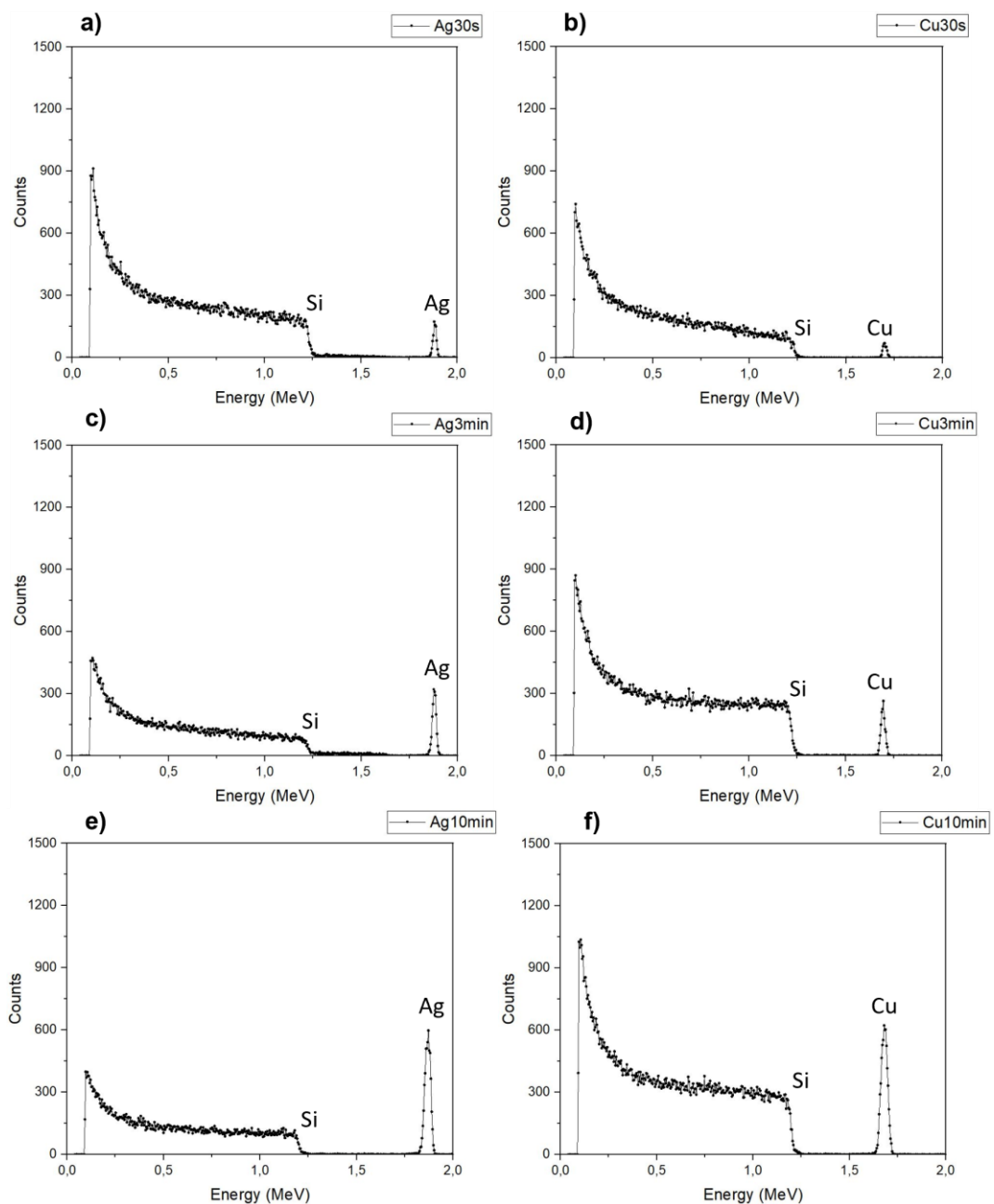
Sample	Element	Deposition Time (s)	Approximate Thickness (nm)
Ag30s	Ag	30	8.5
Ag3min	Ag	180 (3min)	25.2
Ag10min	Ag	600 (10min)	50.7
Cu30min	Ag	1800 (30min)	*
Cu30s	Cu	30	3.5
Cu3min	Cu	180 (3min)	10.4
Cu10min	Cu	600 (10min)	28.6
Cu30min	Cu	1800 (30min)	*

***The thickness of the samples with a deposition time of 30 minutes (Ag30min and Cu30min) could not be estimated due to lack of samples.**

Source: The Author (2022).

The presence of the metallic materials deposited on samples were evaluated and confirmed by RBS measurements. The samples analyzed by RBS were samples with 30 seconds of silver deposition (Ag30s), samples with 3 minutes of silver deposition (Ag3min), samples with 10 minutes of silver deposition (Ag10min), samples with 30s of copper deposition (Cu30s), samples with 3 minutes of copper deposition (Cu3min), and samples with 10 minutes of copper deposition (Cu10min). The RBS spectra of these samples can be visualized on figure 21.

Figure 21. RBS spectra of the samples analyzed.



Source: The Author (2022).

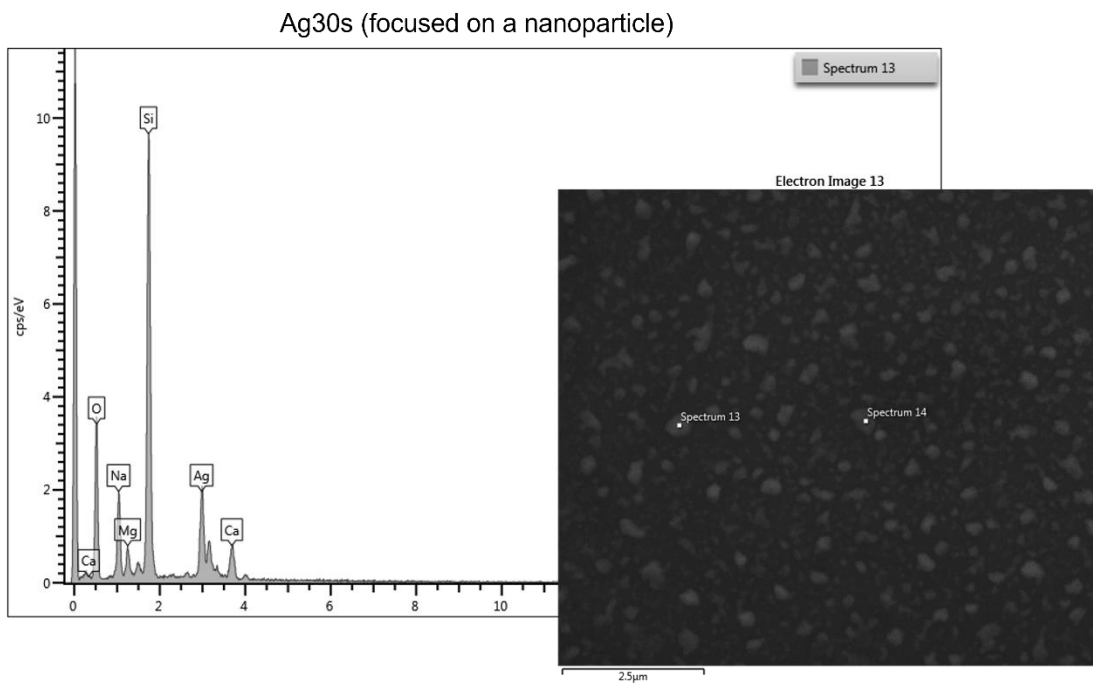
Figure 21 shows RBS spectra where a), c) and e) represent the spectra of samples with deposition times of 30 seconds, 3 minutes, and 10 minutes of silver, respectively. The spectra presented on b), d) and f) are from the samples with deposition times of 30 seconds, 3 minutes, and 10 minutes of copper, respectively. The energy values corresponding to the interaction of the ion beam with the metal particles present on the surface of samples have the same energy values for all silver samples and the same values for all copper samples. What varies is the height of the peaks, that is, the counts. An increase in the height of the peaks is noticed as the thickness of the coatings increases. The energy value for silver coated samples is approximately 1,88MeV and for copper coated samples is approximately 1,7MeV. The atomic mass of copper (63,546 u) is inferior to the atomic mass of silver (107,8682 u) which explains the lower energy value for this element. Also, in figure 21 is possible to observe that the energies do not change with the increase of thickness of the coatings. The silicon (Si) peak corresponds to the substrate material on which the metals were deposited to perform the measurements in the RBS. Si is an element with 28,0855 u of atomic mass, much lighter than Ag and Cu, hence its peak appears at a lower energy level (approximately 1,2 MeV).

The spectra of the samples were simulated in the SIMNRA software using the parameters below.

- Angle of Incidence: 0°;
- Backscatter Angle: 165°;
- Ion Beam Energy: 2 MeV;
- Number of Layers: 2 layers (one layer for the substrate and one for the deposited metallic layer).

From the Energy Dispersive Spectroscopy (EDS) analysis it was possible to evaluate qualitatively the presence of silver and copper on the samples from the generated spectra. Figure 22 represents the spectra of the sample with 30 seconds of silver deposition but focused on a cluster, confirming that the particles that appear in the SEM image are silver nanoparticles.

Figure 22. Spectrum of silver coated sample with 30 seconds of deposition (Ag30s) focused on a silver nanoparticle.



Source: The author (2022).

In addition, semi-quantitative results were also obtained by estimating the atomic and weight percentages of each element present in the samples. Table 4 presents these percentages.

Table 4. Silver and copper percentages analyzed by EDS.

Samples	Ag		Cu	
	Weight (%)	Atomic (%)	Weight (%)	Atomic (%)
Ag30s	3.20	0.61	-	-
Ag3min	32.83	9.62	-	-
Ag10min	81.20	53.39	-	-
Ag30min	100.00	100.00	-	-
Cu30s	-	-	1.07	0.34
Cu3min	-	-	8.85	2.96
Cu10min	-	-	8.48	2.84
Cu30min	-	-	97.37	94.85

Source: The Author (2022).

Table 4 shows the weight and atomic percentages of each metal. The atomic value (%) is the percentage of atoms of Ag or Cu that are present on the sample. The weight value (%) is the element weight percentage. According to the table 4 the weight and atomic values of silver and copper increase as the deposition time increases, what is expected. For Cu3min and Cu10min the percentages showed a different behavior. This may have happened because depending on the area in which the spectrum was recorded, there may be variations in concentrations of the element. Other elements were also identified in the spectra by EDS, such as silicon (Si), calcium (Ca), sodium (Na), magnesium (Mg), aluminum (Al), and oxygen (O). The identification of these elements is due to the composition of the glass substrate. With a thicker coating such as the 30-minute deposition sample, both percentages of silver are 100% and that of copper is near of 100%, because in this case the equipment no longer detects the secondary components related to the substrate so easily.

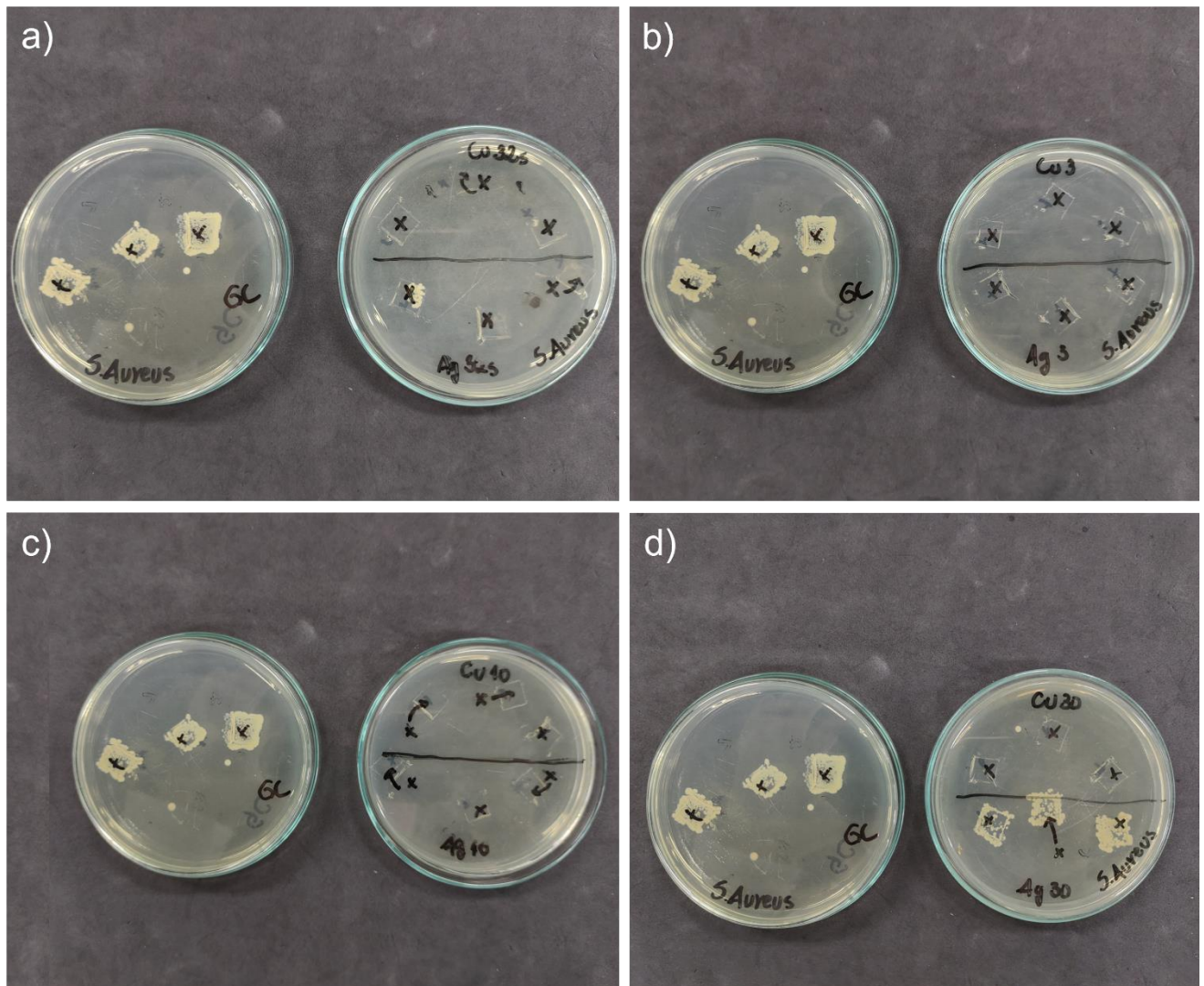
Comparing the values of the samples with silver coating and the samples with copper coating it is possible to notice that the values for the Ag element are higher. For the same deposition times the Ag and Cu elements present different values because the deposition rate of Ag via magnetron sputtering is higher than the deposition rate of Cu. Therefore, for the same deposition time, greater amounts of silver than copper will be obtained. Which justifies the higher percentages related to Ag in table 4.

5.3. Analysis of Antibacterial test

5.3.1. Contact Method

The results of the Contact Method for samples with silver deposition can be visualized in Figure 23.

Figure 23: Contact method test using *S. aureus* for samples with silver and copper deposition and for pure glass samples used as control group.



Source: The author (2022).

Figure 23(a) shows the biological results for the group of samples with no coating – control group (CG) – on the left side of the image, and for copper (Cu30s) and silver (Ag30s) depositions with a deposition time of 30 seconds, on the right side. Figure 23(b) shows the results for GC and for copper (Cu3) and silver (Ag3) depositions with a deposition time of 3 minutes. Figure 23(c) shows the results for GC and for copper (Cu10) and silver (Ag10) depositions with a deposition time of 10

minutes. Figure 23(d) shows the results for GC and for copper (Cu30) and silver (Ag30) depositions with a deposition time of 30 minutes.

The “x” marks on the petri dishes represents the places where the impressions were made. The printing stage is represented in Figure 9(e). Sometimes the sample could not be placed on the exactly “x” mark, hence on some petri dishes there are arrows drawn that indicate a correction of the place where the impression was made. The line on the petri dishes represents the division between the silver samples and copper samples with same deposition times. The bacteria (*S. aureus*) used for this test is identified on the plates as well. It is also possible to observe the marks on the BHI agar caused by the pressure necessary to perform the printing of the square glass samples on the agar.

All the plates positioned on the left side of the figures 23(a), 23(b), 23(c), and 23(d) represent the results obtained for the samples of the control group. The control group comprises the samples that had no coating. For this group of samples (GC) it is possible to visualize that there was a considerable formation of colonies, not being possible to carry out the counting of these colonies. For the test that was applied it is considered a high colonies growth. It is observed that the colony formation occurred in such a manner that the growth assumed the square format of the samples that were printed there. The growth of colonies was limited to the area where there was direct contact of the surface of the samples with BHI agar.

In the upper half of the petri dish positioned on the right side of figure 23(a) are the results obtained for samples with 30 seconds copper deposition (Cu30s). For these samples no bacterial growth was observed. Below, still in figure 23(a), on the same plate, are the results for samples with 30 seconds silver deposition (Ag30s). For these, the growth of colonies was observed only for one specimen of the triplicate. This growth was localized and focused only on one corner of the sample mark on the agar. In the case of this specific sample, there was a detachment of part of the film in the region where the colonies grew. This detachment occurred during the autoclaving process. Therefore, the formation of colonies happened precisely in the part of the sample that was not covered with silver. Apart from that, for all three silver samples with 30s deposition it was observed that there was no bacterial growth, considering that all coated regions of these samples

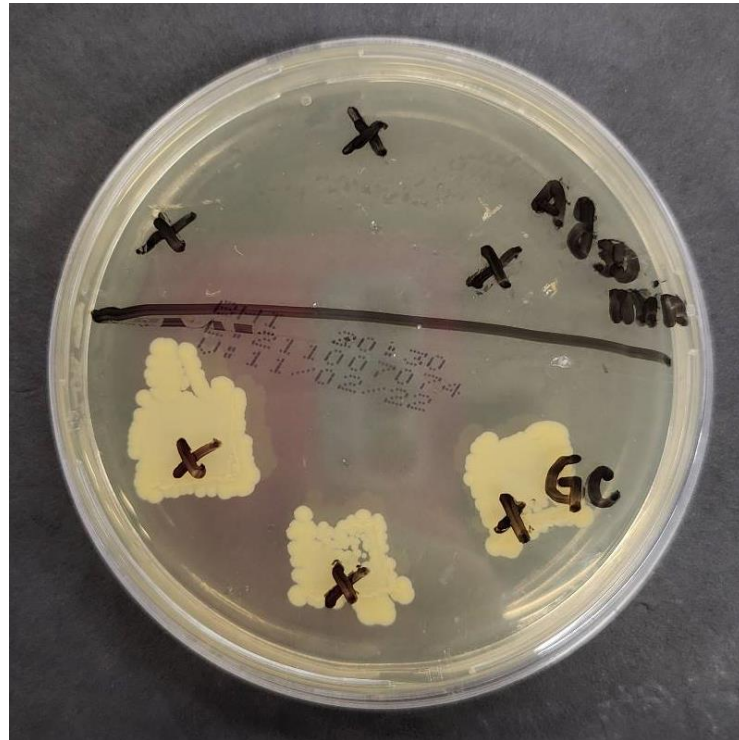
inhibited the formation of colonies. For this group of samples, then, only the region without the coating was observed bacterial growth.

In figure 23(b) the results are shown for samples with a deposition time of 3 minutes. In the upper half of the plate are the silver-coated samples and in the lower half are the copper-coated samples. It is possible to notice that for these two groups of samples (Cu30s and Ag30s) there was no colony formation. Figure 23(c) shows the results of the impressions of the silver and copper samples with a deposition time of 10 minutes for both. The results for the copper coated samples are in the upper part of the petri dish and the silver coated ones are shown in the lower half. No bacterial growth was observed for any of the samples with this deposition time (10min).

Figure 23(d) comprises the results for samples with silver and copper coatings with a deposition time of 30 minutes. On the top half of the petri dish are the results for the impressions of the copper samples and on the bottom half for the silver samples. For the set of samples with copper coating, no bacterial growth was observed. For the triplicate of silver-coated samples, however, it was observed that there was considerable colony formation. Visually, it appears to be a slightly smaller growth than for the samples from the control group, but still a large number of colonies were formed. It was also not possible to perform the colony count for this case.

The second test performed with the samples with 30 minutes silver coating and with a 1:100 dilution presented very different results. These results can be seen in figure 24.

Figure 24. Contact method test with serial dilution of 1:100 using *S. aureus* for samples with silver deposition of 30 minutes and for pure glass samples used as control group.



Source: The author (2022).

For this test the results observed were different from the results found for the contact method with no dilution for the same samples (30 minutes silver deposition). In figure 24 it is possible to visualize that for the control group it has a significant bacterial growth and for the samples with silver coating there was no colony formation. Thus, observing these results it is possible to notice that there was no bacterial growth when the test is performed with a lower density of bacteria. This indicates that the antibacterial action of silver coating with a higher concentration of silver exists, but for lower bacterial densities.

6. CONCLUSIONS

In this work, the antibacterial effect of different thickness of silver and copper coatings on glass were investigated, and the morphology of these coatings was also evaluated. The analysis of samples by Scanning Electron Microscopy showed that for samples with higher deposition times, such as 3 minutes, 10 minutes and 30 minutes, a continuous film is formed and with few imperfections. With shorter deposition times, such as 30 seconds, there is formation of nanoparticles.

It was possible to evaluate the antibacterial effect of the coatings qualitatively, using the contact method. The glass samples with silver and copper coatings showed good results for inhibition of *S. aureus*, even for at the shortest deposition time of 30 seconds. The 30 second-silver coating and 30 second-copper coating keeps the sample with a good level of transparency and present antibacterial effect. For some applications this specific characteristic is important, like face shields.

In the test with 1:100 dilution it was possible to notice that the bacterial growth is dependent on the bacterial density and there is a limit for the antibacterial action of the coating. This relation between the bacterial density and bactericidal agents was not found in most articles testing metallic coatings. Hence, the density of bacteria is an important variable to be studied when dealing with antibacterial coatings.

Therefore, silver and copper coatings produced by the magnetron sputtering deposition method using the parameters applied in this study presented good results as antibacterial agents against *Staphylococcus aureus*. Short time depositions of Ag or Cu produced surfaces with bactericidal action as good as thicker films with higher concentrations of Ag and Cu. Thinking in terms of costs and optical transparency, the coatings with less material (shorter deposition times) are more interesting. The coating with the highest amount of silver was the only one which

showed to be ineffective against *S. aureus* in the first test (high density of bacteria) but showed good antibacterial action for a low density of bacteria.

7. PROPOSALS FOR FUTURE WORK

As next steps of this project, other tests and procedures are planned:

- To perform biological tests with a gram-negative bacterium.
- To explore and evaluate the antibacterial effect for bimetallic samples, producing Ag/Cu coatings with different proportions.
- To evaluate antiviral effect of the coatings.
- Change the substrate to evaluate antibacterial effect for different surfaces with silver and copper coatings.

8. REFERENCES

AHMED, Mohamed K.; AFIFI, Mohamed; USKOKOVIĆ, Vuk. Protecting healthcare workers during COVID-19 pandemic with nanotechnology: A protocol for a new device from Egypt. **Journal Of Infection And Public Health**, v. 13, n. 9, p. 1243-1246, jul. 2020. (Short Communication).

AMERICAN SOCIETY FOR MICROBIOLOGY. Kirby-Bauer Disk Diffusion Susceptibility Test Protocol. 2009. Available in: <https://asm.org/Protocols/Kirby-Bauer-Disk-Diffusion-Susceptibility-Test-Pro>. Access in: May 21, 2021.

BAGHRICHE, O.; RUALES, C.; SANJINES, R.; PULGARIN, C.; ZERTAL, A.; STOLITCHNOV, I.; KIWI, J.. Ag-surfaces sputtered by DC and pulsed DC-magnetron sputtering effective in bacterial inactivation: testing and characterization. **Surface And Coatings Technology**, v. 206, n. 8-9, p. 2410-2416, jan. 2012. Elsevier BV. <http://dx.doi.org/10.1016/j.surfcoat.2011.10.041>. Access in: Apr. 27, 2021.

BALAGNA, Cristina; PERERO, Sergio; PERCIVALLE, Elena; NEPITA, Edoardo V.; FERRARIS, Monica. Virucidal effect against coronavirus SARS-CoV-2 of a silver nanocluster/silica composite sputtered coating. *Open Ceramics*, v. 1, 2020. ISSN 2666-5395. <https://doi.org/10.1016/j.oceram.2020.100006>. Access in: Mar. 03, 2021.

BENETTI, Giulio; CAVALIERE, Emanuele; BANFI, Francesco; GAVIOLI, Luca. Antimicrobial Nanostructured Coatings: a gas phase deposition and magnetron sputtering perspective. *Materials*, v. 13, n. 3, p. 784, 8 fev. 2020. MDPI AG. <http://dx.doi.org/10.3390/ma13030784>. Access in: May 19, 2021.

BERTI, Leandro Antunes; PORTO, Luismar Marques. Nanossegurança : guia de boas praticas em nanotecnologia para fabricaço e laboratorios. Cengage Learning, 2016. 240 p. Access in: May 21, 2021.

CAMPOS, Estefania V. R.; PEREIRA, Anderson E. S.; OLIVEIRA, Jhones Luiz de; CARVALHO, Lucas Bragança; GUILGER-CASAGRANDE, Mariana; LIMA, Renata de; FRACETO, Leonardo Fernandes. How can nanotechnology help to combat COVID-19? Opportunities and urgent need. **Journal Of Nanobiotechnology**, v. 18, n. 1, art. 25, 5 set. 2020. Springer Science and Business Media LLC. <http://dx.doi.org/10.1186/s12951-020-00685-4>. Access in: Apr. 13, 2021.

CARTER, John B.; SAUNDERS, Venetia A. **Virology**: principles and applications. School Of Biomolecular Sciences, Liverpool John Moores University, Uk: John Wiley & Sons, Ltd, 2007. 383 p. Access in: Apr. 12, 2021.

CHU, W.; MAYER, J.; NICOLET, M. Backscattering Spectrometry: Academic Press, New York 1978.

CHUANG, Kuan-Ting; ABDULLAH, Hairus; LEU, Sy-Jye; CHENG, Kou-Bin; KUO, Dong-Hau; CHEN, Hsin-Chieh; CHIEN, Jian-Hao; HU, Wan-Ting. Metal oxide composite thin films made by magnetron sputtering for bactericidal application. **Journal Of Photochemistry And Photobiology A: Chemistry**, v. 337, p. 151-164, mar. 2017. Elsevier BV. <http://dx.doi.org/10.1016/j.jphotochem.2017.01.012>. Access in: Apr. 27, 2021.

CINTEZA, Ludmila; SCOMOROSCENCO, Cristina; VOICU, Sorina; NISTOR, Cristina; NITU, Sabina; TRICA, Bogdan; JECU, Maria-Luiza; PETCU, Cristian. Chitosan-Stabilized Ag Nanoparticles with Superior Biocompatibility and Their Synergistic Antibacterial Effect in Mixtures with Essential Oils. **Nanomaterials**, v. 8, n. 10, p. 826, 13 out. 2018. MDPI AG. <http://dx.doi.org/10.3390/nano8100826>. Access in: Apr. 17, 2021.

CRUZ, Mercedes Cecilia; RUANO, Gustavo; WOLF, Marcus; HECKER, Dominic; VIDAURRE, Elza Castro; SCHMITTGENS, Ralph; RAJAL, Veronica Beatriz. Plasma deposition of silver nanoparticles on ultrafiltration membranes: antibacterial and anti-biofouling properties. **Chemical Engineering Research And Design**, v. 94, p. 524-

537, fev. 2015. Elsevier BV. <http://dx.doi.org/10.1016/j.cherd.2014.09.014>. Access in: Apr. 20, 2021.

DEDAVID, Berenice Anina; GOMES, Carmem Isse; MACHADO, Giovanna. **Microscopia Eletrônica de Varredura: Aplicações e Preparação de Amostras**: materiais poliméricos, metálicos e semicondutores. Porto Alegre: Edipucrs, 2007. 60 p.

DELLA VENTURA, Bartolomeo; CENNAMO, Michele; MINOPOLI, Antonio; CAMPANILE, Raffaele; CENSI, Sergio Bolletti; TERRACCIANO, Daniela; PORTELLA, Giuseppe; VELOTTA, Raffaele. Colorimetric Test for Fast Detection of SARS-CoV-2 in Nasal and Throat Swabs. **Acs Sensors**, v. 5, n. 10, p. 3043-3048, 29 set. 2020. American Chemical Society (ACS). <https://doi.org/10.1021/acssensors.0c01742>. Access in: Apr. 12, 2020.

EREMENKO, A. M.; PETRIK, I. S.; SMIRNOVA, N. P.; RUDENKO, A. V.; MARIKVAS, Y. S.. Antibacterial and Antimycotic Activity of Cotton Fabrics, Impregnated with Silver and Binary Silver/Copper Nanoparticles. **Nanoscale Research Letters**, v. 11, n. 1, p. 1-9, 19 jan. 2016. Springer Science and Business Media LLC. <http://dx.doi.org/10.1186/s11671-016-1240-0>. Access in: Apr. 17, 2020.

FAN, Zhiyuan; DI, Lanbo; ZHANG, Xiuling; WANG, Hongyang. A surface dielectric barrier discharge plasma for preparing cotton-fabric-supported silver nanoparticles. **Nanomaterials**, v. 9, n. 7, p. 961, 01 jul. 2019. Access in: Apr. 26, 2020.

FAUCI, Anthony S.; LANE, H. Clifford; REDFIELD, Robert R. Covid-19 — Navigating the Uncharted. **New England Journal Of Medicine**, v. 382, n. 13, p. 1268-1269, 26 mar. 2020. Semanal. Massachusetts Medical Society. <http://dx.doi.org/10.1056/nejme2002387>. Access in: Apr.12, 2021.

FOUAD, Ghadha Ibrahim. A proposed insight into the anti-viral potential of metallic nanoparticles against novel coronavirus disease-19 (COVID-19). **Bulletin Of The National Research Centre**, v. 45, n. 1, art. 36, 5 fev. 2021. Springer Science and Business Media LLC. <http://dx.doi.org/10.1186/s42269-021-00487-0>. Access in: Apr. 13, 2021.

GALDIERO, Stefania; FALANGA, Annarita; VITIELLO, Mariateresa; CANTISANI, Marco; MARRA, Veronica; GALDIERO, Massimiliano. Silver Nanoparticles as Potential Antiviral Agents. **Molecules**, v. 16, n. 10, p. 8894-8918, 24 out. 2011. MDPI AG. <http://dx.doi.org/10.3390/molecules16108894>. Access in: Apr. 13, 2021.

HORNYAK, Gabor L.; DUTTA, Joydeep; TIBBALS, Harry F.; RAO, Anil K. **Introduction to nanoscience**. Boca Raton: Crc, 2008. 815 p.

HURAIMEL, Khaled Al; ALHOSANI, Mohamed; KUNHABDULLA, Shabana; STIETIYA, Mohammed Hashem. SARS-CoV-2 in the environment: modes of transmission, early detection and potential role of pollutions. **Science Of The Total Environment**, v. 744, p. 140946, nov. 2020. Elsevier BV. <http://dx.doi.org/10.1016/j.scitotenv.2020.140946>. Access in: Apr. 12, 2021.

ILIĆ, Vesna; ŠAPONJIĆ, Zoran; VODNIK, Vesna; LAZOVIĆ, Saša; DIMITRIJEVIĆ, Suzana; JOVANČIĆ, Petar; NEDELJKOVIĆ, Jovan M.; RADETIĆ, Maja. Bactericidal Efficiency of Silver Nanoparticles Deposited onto Radio Frequency Plasma Pretreated Polyester Fabrics. *Industrial & Engineering Chemistry Research*, [S.L.], v. 49, n. 16, p. 7287-7293, 18 ago. 2010. American Chemical Society (ACS). <http://dx.doi.org/10.1021/ie1001313>. Access in: May 20, 2021.

IRFAN, Muhammad; POLONSKYI, Oleksandr; HINZ, Alexander; MOLLEA, Chiara; BOSCO, Francesca; STRUNSKUS, Thomas; BALAGNA, Cristina; PERERO, Sergio; FAUPEL, Franz; FERRARIS, Monica. Antibacterial, highly hydrophobic and semi transparent Ag/plasma polymer nanocomposite coating on cotton fabric obtained by plasma based co-deposition. **Cellulose**, v. 26, n. 16, p. 8877-8894, 16 ago. 2019. Springer Science and Business Media LLC. <http://dx.doi.org/10.1007/s10570-019-02685-6>. Access in: Apr. 27, 2021.

JEREMIAH, Sundararaj S.; MIYAKAWA, Kei; MORITA, Takeshi; YAMAOKA, Yutaro; RYO, Akihide. Potent antiviral effect of silver nanoparticles on SARS-CoV-2. **Biochemical And Biophysical Research Communications**, v. 533, n. 1, p. 195-200, nov. 2020. Elsevier BV. <http://dx.doi.org/10.1016/j.bbrc.2020.09.018>. Access in: Apr. 23, 2021.

JUNG, Sunghoon; YANG, Jun-Yeoung; BYEON, Eun-Yeon; KIM, Do-Geun; LEE, Da-Gyum; RYOO, Sungweon; LEE, Sanggu; SHIN, Cheol-Woong; JANG, Ho Won; KIM, Hyo Jung. Copper-Coated Polypropylene Filter Face Mask with SARS-CoV-2 Antiviral Ability. **Polymers**, v. 13, n. 9, p. 1367, 22 abr. 2021. MDPI AG. <http://dx.doi.org/10.3390/polym13091367>. Access in: Apr. May 01, 2021.

KERRY, Rout George; MALIK, Santosh; REDDA, Yisehak Tsegaye; SAHOO, Sabuj; PATRA, Jayanta Kumar; MAJHI, Sanatan. Nano-based approach to combat emerging viral (NIPAH virus) infection. **Nanomedicine: Nanotechnology, Biology and Medicine**, v. 18, p. 196-220, jun. 2019. Elsevier BV. <http://dx.doi.org/10.1016/j.nano.2019.03.004>. Access in: Apr. 13, 2021.

KHARE, Tushar; OAK, Uttara; SHRIRAM, Varsha; VERMA, Sandeep Kumar; KUMAR, Vinay. Biologically synthesized nanomaterials and their antimicrobial potentials. *Engineered Nanomaterials And Phytonanotechnology: Challenges for Plant Sustainability*, p. 263-289, 2019. Elsevier. <http://dx.doi.org/10.1016/bs.coac.2019.09.002>. Access in: May 21, 2021.

KHEZERLOU, Arezou; ALIZADEH-SANI, Mahmood; AZIZI-LALABADI, Maryam; EHSANI, Ali. Nanoparticles and their antimicrobial properties against pathogens including bacteria, fungi, parasites and viruses. **Microbial Pathogenesis**, v. 123, p. 505-526, out. 2018. Elsevier BV. <http://dx.doi.org/10.1016/j.micpath.2018.08.008>. Access in: Apr. 17, 2021.

KOWALCZYK, Paweł; SZYMCZAK, Mateusz; MACIEJEWSKA, Magdalena; LASKOWSKI, Łukasz; LASKOWSKA, Magdalena; OSTASZEWSKI, Ryszard; SKIBA, Grzegorz; FRANIAK-PIETRYGA, Ida. All That Glitters Is Not Silver—A New Look at Microbiological and Medical Applications of Silver Nanoparticles. **International Journal Of Molecular Sciences**, v. 22, n. 2, p. 854, 16 jan. 2021. MDPI AG. <http://dx.doi.org/10.3390/ijms22020854>. Access in: Apr. 18, 2021.

KUDZIN, Marcin H.; MROZIŃSKA, Zdzisława; KACZMAREK, Anna; LISIAK-KUCIŃSKA, Agnieszka. Deposition of Copper on Poly(Lactide) Non-Woven Fabrics by Magnetron Sputtering—Fabrication of New Multi-Functional, Antimicrobial Composite Materials. **Materials**, v. 13, n. 18, p. 3971, 8 set. 2020. MDPI AG. <http://dx.doi.org/10.3390/ma13183971>. Access in: Apr. 28, 2021.

KUDZIN, Marcin H.; KACZMAREK, Anna; MROZIŃSKA, Zdzisława; OLCZYK, Joanna. Deposition of Copper on Polyester Knitwear Fibers by a Magnetron Sputtering System. Physical Properties and Evaluation of Antimicrobial Response of New Multi-Functional Composite Materials. **Applied Sciences**, v. 10, n. 19, p. 6990, 7 out. 2020. MDPI AG. <http://dx.doi.org/10.3390/app10196990>. Access in: Apr. 28, 2021.

LARA, Humberto H; GARZA-TREVIÑO, Elsa N; IXTEPAN-TURRENT, Liliana; SINGH, Dinesh K. Silver nanoparticles are broad-spectrum bactericidal and virucidal compounds. **Journal Of Nanobiotechnology**, v. 9, n. 1, p. 30, 2011. Springer Science and Business Media LLC. <http://dx.doi.org/10.1186/1477-3155-9-30>. Access in: Apr. 22, 2021.

LEVINSON, Warren. **Microbiologia Médica e Imunologia**. 10. ed. São Francisco (Califórnia): Amgh Editora Ltda., 2011. 676 p. (10). Tradução: Martha Maria Macedo Kyaw. Access in: May 20, 2021.

LI, Geng; FAN, Yaohua; LAI, Yanni; HAN, Tiantian; LI, Zonghui; ZHOU, Peiwen; PAN, Pan; WANG, Wenbiao; HU, Dingwen; LIU, Xiaohong; ZANG, Qiwei; WU, Jianguo. Coronavirus infections and immune responses. **Journal Of Medical Virology**, v. 92, n. 4, p. 424-432, 7 fev. 2020. Wiley. <http://dx.doi.org/10.1002/jmv.25685>. Access in: May 20, 2021.

LIAO, Chengzhu; LI, Yuchao; TJONG, Sie. Bactericidal and Cytotoxic Properties of Silver Nanoparticles. **International Journal Of Molecular Sciences**, v. 20, n. 2, p. 449, 21 jan. 2019. MDPI AG. <http://dx.doi.org/10.3390/ijms20020449>. Access in: Apr. 21, 2021.

LIU, Shangpeng; LI, Jiwei; ZHANG, Shaohua; ZHANG, Xiying; MA, Jianwei; WANG, Na; WANG, Shuang; WANG, Bin; CHEN, Shaojuan. Template-Assisted Magnetron Sputtering of Cotton Nonwovens for Wound Healing Application. **ACS Applied Bio Materials**, v. 3, n. 2, p. 848-858, 24 dez. 2019. American Chemical Society (ACS). <http://dx.doi.org/10.1021/acsabm.9b00942>. Access in: Apr. 27, 2021.

MAGHIMAA, M.; ALHARBI, Sulaiman Ali. Green synthesis of silver nanoparticles from *Curcuma longa* L. and coating on the cotton fabrics for

antimicrobial applications and wound healing activity. **Journal Of Photochemistry And Photobiology B: Biology**, v. 204, p. 111806, mar. 2020. Elsevier BV. <http://dx.doi.org/10.1016/j.jphotobiol.2020.111806>. Access in: Apr. 25, 2021.

MAILLARD, Jean-Yves; HARTEMANN, Philippe. Silver as an antimicrobial: facts and gaps in knowledge. **Critical Reviews In Microbiology**, v. 39, n. 4, p. 373-383, 28 ago. 2012. Informa UK Limited. <http://dx.doi.org/10.3109/1040841x.2012.713323>. Access in: Apr. 20, 2021.

MAYER, M. Rutherford Backscattering Spectrometry (RBS). In: WORKSHOP ON NUCLEAR DATA FOR SCIENCE AND TECHNOLOGY: MATERIALS ANALYSIS, 2003, Trieste. **Lectures. 2003. Access in: May 21, 2021.**

MEI, L.; WANG, J.; WANG, X.; YANG, C.. Antimicrobial activity of Ag surfaces sputtered by magnetron sputtering. **Materials Research Innovations**, v. 18:sup4, p. S4875-S4878, jul. 2014. Informa UK Limited. <http://dx.doi.org/10.1179/1432891714z.000000000806>. Access in: Apr. 27, 2021.

MEISTER, T.L., FORTMANN, J., BREISCH, M. *et al.* Nanoscale copper and silver thin film systems display differences in antiviral and antibacterial properties. *Sci Rep* **12**, 7193 (2022). <https://doi.org/10.1038/s41598-022-11212-w>

MELO, Celso Pinto de; PIMENTA, Marcos. Nanociências e Nanotecnologia. **Parcerias Estratégicas**, Brasília, v. 9, n. 18, p. 9-21, 2004. http://seer.cgee.org.br/index.php/parcerias_estrategicas/article/view/130. Access in: Feb. 17, 2021.

MENG, Lingling; WANG, Youjiang; WEI, Qufu; HUANG, Xinmin; SHEN, Jiayu; CHEN, Hongwei. Study on the structure and properties of Ag/Cu nanocomposite film deposited on the surface of polyester substrates. **The Journal Of The Textile Institute**, p. 1-7, 23 out. 2020. Informa UK Limited. <http://dx.doi.org/10.1080/00405000.2020.1838129>. Access in: May 03, 2021.

PARKER, Nina; SCHNEEGURT, Mark; TU, Anh-Hue Thi; FORSTER, Brian M.; LISTER, Philip. **Microbiology**. Rice University, Houston, Texas: Asm Press/Openstax, 2016. 1317 p. Access in: Apr.12, 2021.

PATRA, Jayanta Kumar; DAS, Gitishree; FRACETO, Leonardo Fernandes; CAMPOS, Estefania Vangelie Ramos; RODRIGUEZ-TORRES, Maria del Pilar; ACOSTA-TORRES, Laura Susana; DIAZ-TORRES, Luis Armando; GRILLO, Renato; SWAMY, Mallappa Kumara; SHARMA, Shivesh; HABTEMARIAM, Solomon; SHIN, Han-Seung. Nano based drug delivery systems: recent developments and future prospects. **Journal Of Nanobiotechnology**, v. 16, n. 1, art. 71, 19 set. 2018. Springer Science and Business Media LLC. <http://dx.doi.org/10.1186/s12951-018-0392-8>. Access in: Apr. 13, 2021.

POGGIO, Claudio; COLOMBO, Marco; ARCIOLA, Carla Renata; GREGGI, Tiziana; SCRIBANTE, Andrea; DAGNA, Alberto. Copper-Alloy Surfaces and Cleaning Regimens against the Spread of SARS-CoV-2 in Dentistry and Orthopedics. From Fomites to Anti-Infective Nanocoatings. **Materials**, v. 13, n. 15, p. 3244, 22 jul. 2020. MDPI AG. <http://dx.doi.org/10.3390/ma13153244>. Access in: Apr. 24, 2021.

PRESCOTT, Lansing M.; HARLEY; KLEIN. **Microbiology**. 5. ed. McGraw-Hill Higher Education, 2002. 1147 p.

RAFFI, Muhammad; MEHRWAN, Saba; BHATTI, Tariq Mahmood; AKHTER, Javed Iqbal; HAMEED, Abdul; YAWAR, Wasim; HASAN, M. Masood Ul. Investigations into the antibacterial behavior of copper nanoparticles against Escherichia coli. **Annals Of Microbiology**, v. 60, n. 1, p. 75-80, 17 fev. 2010. Springer Science and Business Media LLC. <http://dx.doi.org/10.1007/s13213-010-0015-6>. Access in: Apr. 24, 2021.

RAI, Mahendra; DESHMUKH, Shivaji D.; INGLE, Avinash P.; GUPTA, Indarchand R.; GALDIERO, Massimiliano; GALDIERO, Stefania. Metal nanoparticles: the protective nanoshield against virus infection. **Critical Reviews In Microbiology**, v. 42, n. 1, p. 46-56, 22 abr. 2014. Informa UK Limited. <http://dx.doi.org/10.3109/1040841x.2013.879849>. Access in: Apr. 17, 2021.

SCHUMACHER, A.; VRANKEN, T.; MALHOTRA, A.; ARTS, J. J. C.; HABIBOVIC, P.. In vitro antimicrobial susceptibility testing methods: agar dilution to 3d tissue-engineered models. **European Journal Of Clinical Microbiology & Infectious**

Diseases, v. 37, n. 2, p. 187-208, 4 set. 2017. Springer Science and Business Media LLC. <http://dx.doi.org/10.1007/s10096-017-3089-2>. Access in: May 21, 2021.

SHAHIDI, Sheila; GHORANNEVISS, Mahmood. Plasma Sputtering for Fabrication of Antibacterial and Ultraviolet Protective Fabric. **Clothing And Textiles Research Journal**, v. 34, n. 1, p. 37-47, 9 jul. 2015. SAGE Publications. <http://dx.doi.org/10.1177/0887302x15594455>. Access in: Apr. 27, 2021.

SHANKAR, Shiv; RHIM, Jong-Whan. Facile approach for large-scale production of metal and metal oxide nanoparticles and preparation of antibacterial cotton pads. **Carbohydrate Polymers**, v. 163, p. 137-145, maio 2017. Elsevier BV. <http://dx.doi.org/10.1016/j.carbpol.2017.01.059>. Access in: Apr. 17, 2021.

SINGH, Lavanya; KRUGER, Hendrik G.; MAGUIRE, Glenn E.M.; GOVENDER, Thavendran; PARBOOSING, Raveen. The role of nanotechnology in the treatment of viral infections. **Therapeutic Advances In Infectious Disease** v. 4, n. 4, p. 105-131, 2017.

SPORTELLI, Maria Chiara; IZZI, Margherita; KUKUSHKINA, Ekaterina A.; HOSSAIN, Syed Imdadul; PICCA, Rosaria Anna; DITARANTO, Nicoletta; CIOFFI, Nicola. Can Nanotechnology and Materials Science Help the Fight against SARS-CoV-2? **Nanomaterials**, v. 10, n. 4, p. 802, 21 abr. 2020. MDPI AG. <http://dx.doi.org/10.3390/nano10040802>. Access in: May 20, 2021.

SUBRAMANIAN, B.; PRIYA, K. Anu; RAJAN, S. Thanka; DHANDAPANI, P.; JAYACHANDRAN, M.. Antimicrobial activity of sputtered nanocrystalline CuO impregnated fabrics. **Materials Letters**, v. 128, p. 1-4, ago. 2014. Elsevier BV. <http://dx.doi.org/10.1016/j.matlet.2014.04.056>. Access in: May 02, 2021.

TUDOSE, Ioan Valentin; COMANESCU, Florin; PASCARIU, Petronela; BUCUR, Stefan; RUSEN, Laurentiu; IACOMI, Felicia; KOUDOUMAS, Emmanuel; SUCHEA, Mirela Petruta. Chemical and physical methods for multifunctional nanostructured interface fabrication. **Functional Nanostructured Interfaces For Environmental And Biomedical Applications**, p. 15-26, 2019. Elsevier. <http://dx.doi.org/10.1016/b978-0-12-814401-5.00002-5>. Access in: May 19, 2021.

TORTORA, Gerard J; FUNKE, Berdell R; CASE, Christine L. **Microbiology: an introduction**. 11. ed. Pearson, 2013. 975 p. Access in: May 20, 2021.

WANG, Mei-Yue; ZHAO, Rong; GAO, Li-Juan; GAO, Xue-Fei; WANG, De-Ping; CAO, Ji-Min. SARS-CoV-2: structure, biology, and structure-based therapeutics development. **Frontiers In Cellular And Infection Microbiology**, v. 10, p. 724, 25 nov. 2020. Frontiers Media SA. <http://dx.doi.org/10.3389/fcimb.2020.587269>. Access in: Apr. 12, 2021.

WEBSTER, Thomas J; SEIL, Iustin. Antimicrobial applications of nanotechnology: methods and literature. **International Journal Of Nanomedicine**, p. 2767, jun. 2012. Informa UK Limited. <http://dx.doi.org/10.2147/ijn.s24805>. Access in: Apr. 17, 2021.

Wiegand, I., Hilpert, K. & Hancock, R. Agar and broth dilution methods to determine the minimal inhibitory concentration (MIC) of antimicrobial substances. *Nat Protoc* 3, 163–175 (2008). <https://doi.org/10.1038/nprot.2007.521>

WIEGAND, Irith; HILPERT, Kai; HANCOCK, Robert e W. Agar and broth dilution methods to determine the minimal inhibitory concentration (MIC) of antimicrobial substances. *Nature Protocols*. v. 3, n. 2, p. 163-175, 17 jan. 2008. Springer Science and Business Media LLC. <http://dx.doi.org/10.1038/nprot.2007.521>. Access in: May 21, 2021.

WITTKÄMPER, Florian; BIKOWSKI, André; ELLMER, Klaus; GÄRTNER, Konrad; WENDLER, Elke. Energy-Dependent RBS Channelling Analysis of Epitaxial ZnO Layers Grown on ZnO by RF-Magnetron Sputtering. **Crystals**, v. 9, n. 6, p. 290, 4 jun. 2019. MDPI AG. <http://dx.doi.org/10.3390/cryst9060290>. Access in: May 21, 2021.

WORLD HEALTH ORGANIZATION. WHO Coronavirus (COVID-19) Dashboard. 2021. Available in: <https://covid19.who.int/>. Access in: May 20, 2021.

ZOWALATY, Mohamed El; IBRAHIM, Nor Azowa; SALAMA, Mohamed; SHAMELI, Kamyar; USMAN, Muhammad; ZAINUDDIN, Norhazlin. Synthesis, characterization, and antimicrobial properties of copper nanoparticles. **International**

Journal Of Nanomedicine, p. 4467, nov. 2013. Informa UK Limited.
<http://dx.doi.org/10.2147/ijn.s50837>. Access in: Apr. 24, 2021.



Pontifícia Universidade Católica do Rio Grande do Sul
Pró-Reitoria de Pesquisa e Pós-Graduação
Av. Ipiranga, 6681 – Prédio 1 – Térreo
Porto Alegre – RS – Brasil
Fone: (51) 3320-3513
E-mail: propesq@pucrs.br
Site: www.pucrs.br